Energy & Environmental Science

Cite this: *Energy Environ. Sci.*, 2011, **4**, 2682

www.rsc.org/ees

REVIEW

Recent developments in nanostructured anode materials for rechargeable lithium-ion batteries

Liwen Ji,† Zhan Lin,† Mataz Alcoutlabi and Xiangwu Zhang*

Received 22nd November 2010, Accepted 22nd March 2011
DOI: 10.1039/c0ee00699h

In this paper, the use of nanostructured anode materials for rechargeable lithium-ion batteries (LIBs) is reviewed. Nanostructured materials such as nano-carbons, alloys, metal oxides, and metal sulfides/nitrides have been used as anodes for next-generation LIBs with high reversible capacity, fast power capability, good safety, and long cycle life. This is due to their relatively short mass and charge pathways, high transport rates of both lithium ions and electrons, and other extremely charming surface activities. In this review paper, the effect of the nanostructure on the electrochemical performance of these anodes is presented. Their synthesis processes, electrochemical properties, and electrode reaction mechanisms are also discussed. The major goals of this review are to give a broad overview of recent scientific researches and developments of anode materials using novel nanoscience and nanotechnology and to highlight new progresses in using these nanostructured materials to develop high-performance LIBs. Suggestions and outlooks on future research directions in this field are also given.

1. Introduction

Rechargeable lithium-ion batteries (LIBs) have been considered as the most promising energy storage system for a wide variety of applications. LIBs have revolutionized portable electronic devices including cell phones, laptops, and digital cameras with the worldwide market now valued at ten billion dollars.[1–5] They are also important power sources for future electric vehicles, hybrid electric vehicles, and emerging smart grids.[6–16] Rechargeable LIBs offer energy densities 2-3 times and power densities 5-6 times higher than Ni–MH, Ni–Cd, and Pb acid batteries. Rechargeable LIBs have many other advantages such as long cycle life, low self-discharge, high operating voltage, wide temperature window, and no "memory effect". Nowadays, rechargeable LIBs are constructed with various shapes (*e.g.*, cylindrical, coin, or prismatic shapes) by employing different electrode materials.

The charge/discharge mechanism of LIBs is based on the rocking-chair concept. A typical LIB consists of a cathode (*e.g.*, $LiCoO_2$) and an anode (*e.g.*, graphite), together with an electrolyte-filled separator that allows lithium (Li) ion transfer but prevents electrodes from direct contact (Fig. 1). When the battery is charging, Li deintercalates from the cathode and intercalates into the anode. Conversely, Li intercalates into the cathode *via* the electrolyte during discharging. During charge/discharge, Li ions flow between the anode and the cathode, enabling the conversion of chemical energy into electrical energy and the storage of electrochemical energy within the battery.[17–20] The chemical reactions involved in a typical LIB cell are described as follows:

Fiber and Polymer Science Program, Department of Textile Engineering, Chemistry and Science, North Carolina State University, Raleigh, NC, 27695-8301, USA. E-mail: xiangwu_zhang@ncsu.edu; Fax: +1 919-515-6532; Tel: +1 919-515-6547
† These authors contributed equally to this work.

Broader context

Recent progresses in advanced nanoscience and nanotechnology have presented the opportunity to design a series of novel nanostructured anode materials for next-generation high-performance rechargeable lithium-ion batteries (LIBs). Nanostructure-based anodes offer controllable surface area, short mass and charge diffusion distance, and high freedom for volume change during charge-discharge cycles, and hence they can improve the energy density, life cycle and rate capability of LIBs. The major goals of this review article are to highlight the new progresses in using these nanostructured materials as anode electrodes to develop LIBs with high energy density, high rate capability, and excellent cycling stability, and to give a broad picture of recent scientific research in the developments of anode materials from nanoscience and nanotechnology.

Anode:

$$6C + xLi^+ + xe^- \leftrightarrow Li_x C_6 \quad (1)$$

Cathode:

$$LiCoO_2 \leftrightarrow Li_{1-x} CoO_2 + xLi^+ + xe^- \quad (2)$$

The performance of rechargeable LIBs depends on active materials employed for Li storage in the electrodes. The basic requirements for active materials include high reversible capacity, good structural flexibility and stability, fast Li ion diffusion, long cycle life, improved safety, low cost, and environmental benignity.[21–23] In commercial LIBs, cathodes are mainly made from Li-ion host materials possessing high positive redox potentials such as $LiCoO_2$, $LiMn_2O_4$, and recently $LiFePO_4$.[24–26] Graphite is the most used commercial anode material for LIBs because of its low and flat working potential, long cycle life, and low cost. However, the most Li-enriched intercalation compound of graphite has a stoichiometry of LiC_6, resulting in a less-than-desirable theoretical charge capacity (372 mAh g^{-1}) and a small practical energy density.[27,28] Furthermore, the Li-ion transport rates of graphite anodes are always less than 10^{-6} cm^2 s^{-1}, which results in a low power density of the battery since the chemical diffusion coefficient of Li ions is related to the power density of the battery.[29]

In order to improve the energy and power densities of LIBs, the use of anode materials with larger capacities and higher Li diffusion rates is required. Different microscale materials such as pyrolytic carbons, alloys, and metal oxides have been developed as anodes for LIBs. However, further advances in current LIBs

Liwen Ji

Liwen Ji received his B.S. degree in Materials Chemistry from Lanzhou University in 2001 and M.S. degree in Polymer Chemistry and Physics from Zhejiang University in 2004. After nearly two and a half years' research experience in Shanghai Institute of Organic Chemistry, he started to study at North Carolina State University and received his Ph.D. degree in Fiber and Polymer Science in 2009 under the supervision of Professor Xiangwu Zhang. He is currently a Materials Postdoctoral Fellow at the Molecular Foundry, Lawrence Berkeley National Laboratory. His research focuses on novel nanostructures for advanced energy storage and conversion systems.

Mataz Alcoutlabi

Mataz Alcoutlabi received his B. S. degree in Mechanical Engineering from the University of Aleppo, Syria and M.S. degree in Mechanical Engineering from the Institut National des Sciences Appliquées (INSA) de Toulouse, France. He obtained his Ph.D. degree in Materials Science and Engineering from INSA, Lyon, France. After working as a post doctoral researcher at Laval University, Quebec, Canada and at Texas Tech University, he joined the University of Utah in Salt Lake City as a research professor. He is currently a Research Assistant Professor in the College of Textiles at North Carolina State University.

Zhan Lin

Zhan Lin received his B.S. degree in Polymer Science and Engineering from Hefei University of Technology in 2003 and M.S. degree in Applied Chemistry from University of Science and Technology of China in 2006. In 2010, he obtained his Ph.D. degree in Fiber and Polymer Science at North Carolina State University under the direction of Professors Xiangwu Zhang and Wendy E. Krause, focusing on the research areas of lithium-ion batteries and fuel cells. He is currently a Research Associate Postdoctoral in Materials Science and Technology Division at Oak Ridge National Laboratory, working on lithium-sulfur and lithium-ion batteries.

Xiangwu Zhang

Professor Xiangwu Zhang received his B.S. degree in Polymer Materials and Engineering in 1997 and Ph.D. degree in Materials Science and Engineering in 2001, both from Zhejiang University, China. He joined the Center for Electrochemical Systems and Hydrogen Research at Texas A&M University as a Postdoctoral Associate in 2001. During 2002–2006, he was a Postdoctoral Associate in the Department of Chemical and Biomolecular Engineering at North Carolina State University (NCSU). He joined the faculty in the College of Textiles at NCSU in 2006. Zhang's research interests focus on nanostructured and multifunctional materials for energy storage and conversion.

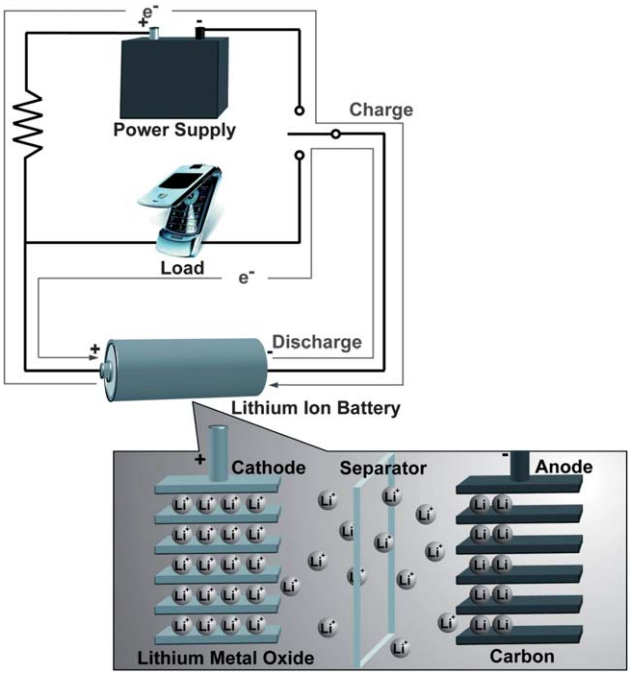

Fig. 1 Schematic operating principle of a typical rechargeable LIBs.

are bottlenecked by limitations associated with these microscale materials such as small surface areas, slow solid-state Li diffusion rates, high electronic resistances, and poor shape flexibilities along with huge morphological and structural changes during charge-discharge processes. As a result, current microscale structured anode materials still suffer from poor cycling stability and unsatisfactory charge/discharge capacities, especially at high current rates. Recent progresses in electrochemistry, nanotechnology, and solid state chemistry have led to the application of nanomaterials for efficient energy storage in high-performance LIBs because of their unique morphologies and structures. Nanomaterials with large surface areas and numerous active sites can be developed to increase the anode capacities and subsequently energy densities of the batteries due to their large spaces and active sites for Li intercalation/deintercalation reactions. In addition, nanomaterial-based electrodes with stable and thin solid electrolyte interface (SEI) films and large electrode/electrolyte contact areas can increase the charge-discharge rates and subsequently power densities because of their effective transfer pathways for both Li ions and electrons. Nanomaterials with flexible structures can also be developed to improve the cycling performance due to sufficient free spaces to relax the large volume changes during continuous charge/discharge reactions. Furthermore, nanostructured composite anode materials containing conductive matrices, such as carbon components, can decrease the interface resistances leading to higher specific capacities at high charge/discharge rates.[30–37]

There have been many review articles on rechargeable LIBs,[38–46] however, there are few comprehensive reviews to cover a large variety of nanostructured anode materials. This review article aims to meet this need by summarizing recent progresses in the synthesis and characterization of nanostructured anode materials for rechargeable LIBs, primarily focusing on nanocarbons, alloys, metal oxides, and metal sulfides/nitrides. For each material, the basic structural and electrochemical properties are described firstly, and then different synthesis approaches and strategies are discussed to indicate how to control the nanostructures and how to improve the electrochemical performance. The electrochemical performance characteristics such as charge/discharge capacity, cycling performance, and rate capability, are discussed for each nanostructured anode material. An overlook on future developments is also presented.

2. Nano-carbons

Carbonaceous materials, especially graphite, are the most used anode materials for rechargeable LIBs. They can avoid the problem of Li dendrite formation by reversible intercalation of Li into carbon host lattice, and this provides good cyclability and safety for LIB anodes. However, graphite has a limited theoretical capacity of 372 mAh g^{-1} since the most Li-enriched intercalation compound of graphite only has a stoichiometry of LiC_6. To increase the energy and power densities of LIBs, nanostructured carboneous anode materials, such as one-dimensional (1D), two-dimensional (2D), and porous carbon-based anodes, have been developed to create more active spaces or sites for Li storage.

2.1. One-dimensional carbon

The development of 1D nanostructured carbon materials, such as nanotubes, nanowires, and nanofibers, for high-performance LIBs is stimulated by their high surface-to-volume ratios and excellent surface activities. Shortly after the discovery of carbon nanotubes (CNTs),[47] researchers studied the interactions of Li vapor with CNTs and measured the corresponding electrochemical properties.[48] It was found that CNTs can offer Li intercalation between pseudo-graphitic layers and/or inside central tubes. The small diameters of CNTs can impose strain on the planar bonds of the hexagon. This strain causes de-localization of electrons and makes the structure more electronegative than regular graphitic sheets, which in return increases the degree of Li intercalation. Therefore, the reversible capacity of anodes made from CNTs can exceed 460 mAh g^{-1} and reach up to 1116 mAh g^{-1} by various post-treatments such as ball milling,[49] acid oxidation,[50] and metal oxide cutting.[51] The relatively high capacity of CNTs represents a dramatic improvement over graphite; however, the Coulombic efficiency of CNTs was found to be low compared with that of graphite due to the introduction of large structure defects[52] and high voltage hysteresis.[53] Various CNTs have been used as anodes for rechargeable LIBs, such as bamboo-shaped CNTs[54] and CNTs with a quadrangular cross section (q-CNTs).[55] The Columbic efficiency of these anodes was improved by the high Li intercalation on the CNT walls, fast electron transfer rate, and the large number of electroactive sites.[55–59]

Carbon nanofibers (CNFs), which were synthesized by many methods such as chemical vapor deposition, arc-discharge, template deposition, laser ablation, and electrospinning, have also been used as anodes for rechargeable LIBs.[60–63] Unlike CNTs, which require a long diffusion time for Li intercalation/deintercalation, a large amount of defects in CNFs such as lattice and surface defects along the fiber length are expected to

promote fast Li intercalation/deintercalation.[61,64,65] More recently, CNF-based anodes were also prepared using the simple and low cost electrospinning technique and subsequent carbonization processes.[66] Electrospun CNF anode materials can deliver a relatively large reversible capacity of approximately 450 mAh g^{-1} at 30 mA g^{-1}. Zhang's group improved the electrochemical performance of CNFs by preparing porous CNFs *via* the electrospinning/carbonization process combined with chemical treatments.[67–69] These porous CNFs had much higher specific surface area and larger pore volume than non-porous CNF anodes. The porous structure improved Li ion diffusion at the electrolyte-electrode interface and added freedom for volume change associated with Li intercalation.

2.2. Two dimensional carbon

Graphene, a novel 2D aromatic monolayer of honeycomb carbon lattice, has also attracted attention for use as an anode material in rechargeable LIBs because of its fascinating physical, chemical, and mechanical properties, such as ultrahigh surface area, intriguing electronic and thermal conductivities, structural flexibility, unique porous structure, and broad electrochemical window.[70–75] In addition, graphene has a considerable Li-storage ability, since Li can be bound not only on both sides of graphene sheets, but also on the edges, defects, disorders, and covalent sites of graphene nanoplatelets. Therefore, it is expected by many researchers that graphene and graphene-based nanocomposites can overtake its 3D counterpart (graphite) for enhanced Li storage in rechargeable LIBs.[76–79] Recently, electrochemical Li intercalation in graphene materials has been explored by several research groups.[70–79] For example, Song *et al.* used chemically prepared graphenes as anodes for rechargeable LIBs to evaluate their electrochemical behavior.[80] These 2D carbon anodes delivered first-cycle charge and discharge capacities of 1233 mAh g^{-1} and 672 mAh g^{-1}, respectively. Although the Coulombic efficiency was low (55%), the reversible capacity still can be preserved at about 502 mAh g^{-1} after 30 cycles. Several other groups also demonstrated that graphene-based anode materials had large charge/discharge capacities along with low initial Coulombic efficiency and large irreversible capacity. The high irreversible capacity of graphene anodes could be explained by the reaction of Li ions with oxygen-containing functional groups and the formation of SEI in nanocavities/defects derived from the wrinkle/oxidation of the graphene.[70–79] In additoin, the electrolyte intercalation into the graphene layers is high because of the large surface-to-volume ratio, which also contributes to the increased irreversible capacity.[80,81]

Graphenes anchored with active metal (*e.g.*, Sn,[82] Sn–Sb,[83] and Si[84]) and/or metal oxide (*e.g.*, Co_3O_4,[85,86] TiO_2,[87] Fe_3O_4,[88,89] Mn_3O_4,[90] CuO,[91] and SnO_2[92]) nanoparticles can be used to reduce the irreversible capacity and enhance the cycle life. For example, Honma *et al.* obtained SnO_2-graphene nanocomposites (Fig. 2a) by reassembling graphene nanosheets in ethylene glycol with the presence of SnO_2 nanoparticles.[93] The existence of SnO_2 nanoparticles prevented the reassembly of graphene to graphite platelets during cycling. It was found that these SnO_2/graphene electrodes exhibited a high reversible capacity of 810 mAh g^{-1} at 50 mA g^{-1}. After 30 cycles, the capacity was preserved at 570 mAh g^{-1}, indicating a 70% capacity retention (Fig. 2b).

The performance enhancement of graphene by forming nanocomposites with metals or metal oxides can be ascribed to several factors. Firstly, both metal/metal oxide nanoparticles and graphene sheets have large Li-storage abilities. Secondly, graphene components have excellent electrical conductivity which ensures good electrical contact between adjacent active particles. Thirdly, the flexible and electronic conductive graphene nanosheets suppress the large volume expansion/extraction of the electrodes during charge/discharge, alleviating the aggregation and pulverization problems connected with pure metal or metal oxide nanoparticles. Finally, the confining of metal or metal oxide nanoparticles between graphene nanosheets mitigates the restacking of graphene sheets, and consequently keeps their high active surface areas and creates more significant disorder/defects and cavities for Li storage. Therefore, these synergic effects of graphene and metal or metal oxide nanoparticles lead to increased Li storage capacity, improved cycling performance, and good rate capability of the graphene/metal and graphene/metal oxide nanocomposites.[82–92]

2.3. Porous carbon

Porous carbons with different pore sizes ranging from nanometre to micrometre scale are promising anode materials for LIBs due to their high surface areas and open pore structures. The desirable characteristics of these materials are the effective diffusion pathways for Li ions due to the formation of percolation networks from interconnected nanopores, reasonable electrical conductivity provided by the well-interconnected carbon walls, large amount of active sites for Li storage, and minimized mechanical stress for volume expansion/contraction during Li intercalation/deintercalation. Because of these unique merits, porous carbons often show prominently increased capacities in comparison with traditional graphitic carbons.[94,95,96]

There are three types of porous carbons, *i.e.*, microporous (pore size < 2 nm), mesoporous (2 nm < pore size < 50 nm), and macroporous (pore size > 50 nm) carbons. Among them, microporous carbons have demonstrated larger capacities than traditional graphitic carbons, although in many cases high irreversibilities are also accompanied.[96] For example, Takeuchi *et al.* used a template method to prepare high-surface area microporous carbons for use as anodes.[97] The results showed a reversible capacity of 480 mAh g^{-1} and a large irreversible capacity of 3685 mAh g^{-1}.[96] This high irreversible capacity was caused by the increased surface area of the microporous carbon which led to an increased SEI area. The large irreversible capacity might also be due to the reactions of Li ions with the surface functional groups (–C=O or –OH) on carbon. Because of the high surface area of these materials, there are many sites for the formation of these functional groups.[44,45] In addition, a high capacity fade was observed in the first few cycles, which further hinders the use of these materials as anodes for LIBs.

Mesoporous carbons (2 nm < pore size < 50 nm) have also been used as anode materials for LIBs.[98] Using silica SBA-15 as a template, Zhou *et al.* synthesized 3D ordered mesoporous carbon materials with uniform pore sizes, high surface areas, and large pore volumes (Fig. 3a).[99] The results (Fig. 3b) showed that at the first cycle the reversible capacity and irreversible capacity were 1100 and 2000 mAh g^{-1}, respectively. After the first cycle,

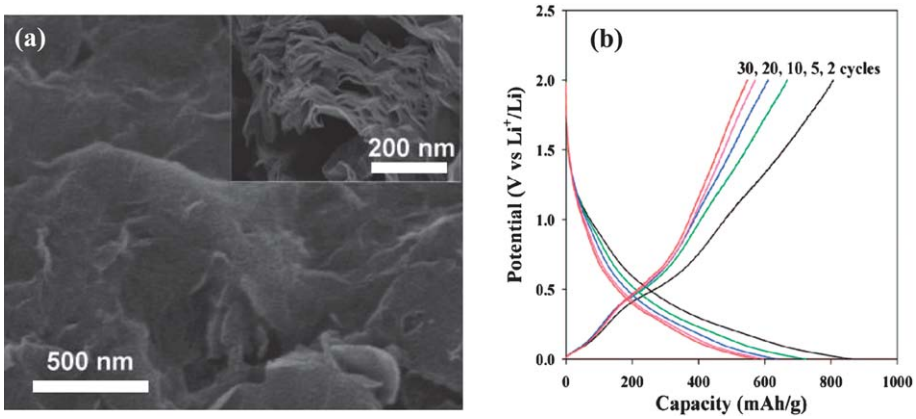

Fig. 2 (a) SEM images, and (b) charge/discharge profile of SnO_2/graphene nanocomposite. Reproduced with permission.[93]

both the charge and discharge capacities remained unchanged. This could be due to the minimized ion transport resistance and localized graphitic structures around the pores and more importantly, to the ordered porous structure.[96,99]

Ordered macroporous carbons (pore size > 50 nm) have also been synthesized by template-based methods. Colloidal suspensions of poly(methyl methacrylate) (PMMA) and inverse silica opal were used as templates by Su *et al.* to prepare ordered macroporous carbons.[100] The resultant anodes exhibited a high capacity of 320 mAh g^{-1} after 60 cycles with a high capacity retention of 98%. Macroporous CNFs with well-interconnected pore and wall structures were prepared by Stein *et al.* using a PMMA colloididal-crystal template.[101] These anodes delivered a capacity of 260 mAh g^{-1} at a current density of 1000 mA g^{-1} with a capacity retention of 83% after 30 cycles.

In summary, the electrochemical performance of nano-carbons (1D, 2D, and porous carbons) is largely determined by their structures and morphologies. The 1D nanostructured carbons have high Coulombic efficiency and good cycling stability. However, they often show unsatisfactory rate performance and low volumetric energy density due to the formation of large SEI films and less-compact structure. In comparison, due to the unique 2D aromatic monolayer of honeycomb carbon lattice, 2D graphene typically shows good rate capability, *i.e.*, small capacity fading even at high rates.[79,102,103] However, graphene-based anodes have relatively low initial Coulombic efficiency and large irreversible capacity due to the reactions between Li ions with oxygen-containing functional groups and to the formation of SEI films in nanocavities/defects. Similar to graphene, porous carbons have low volumetric energy density and large irreversible capacity although their capacity is typically large. Combining different nano-carbons, such as CNT/CNFs[104] or CNF/graphene platelet, could lead to novel carbon nanostructures with improved electrochemical performance. Moreover, hybridising nano-carbons with other high-capacity components (*e.g.*, alloys and/or metal oxides) also offers a promising strategy for achieving excellent overall performance.

3. Alloys

Li can be electrochemically alloyed with a number of metallic and semi-metallic elements in groups IV and V, such as Si, Sn, Ge, Pb, P, As, Sb, and Bi, and also some other metal elements, such as Al, Au, In, Ga, Zn, Cd, Ag, and Mg.[105–107] The Li alloying could be carried out before or during the preparation of the electrodes, but more often it is realized by the charging process after assembling the LIBs. These alloyed anodes are well-known for high specific capacities, moderate operation potentials *vs.* Li/Li^+, and good safety. The main challenge for the implementation of these anodes is the large volume change during Li alloying/dealloying processes. The large volume change causes severe cracking and crumbling of the electrodes and subsequent

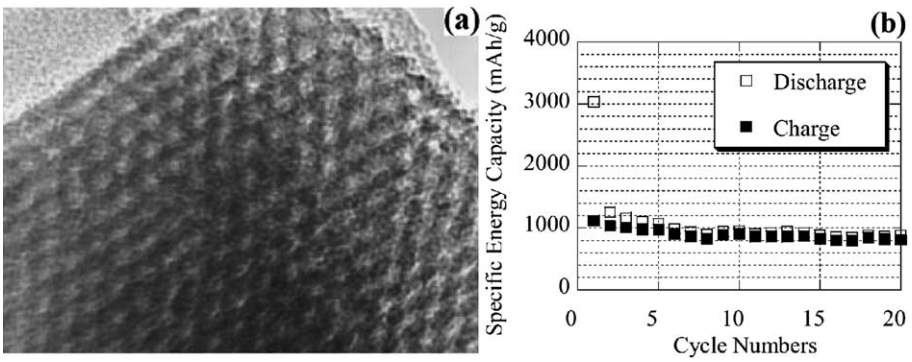

Fig. 3 (a) TEM image of ordered mesoporous carbon perpendicular to the direction of hexagonal pore arrangement, and (b) discharge and charge performance of the ordered mesoporous carbon anode at 100 mA g^{-1}. Reproduced with permission.[99]

loss of electrical contact between individual particles, which in turn results in large irreversible capacity and severe capacity fading.[105–109]

Several strategies have been investigated to overcome the large volume change and preserve the structural integrity. The first approach involves preparing unique nanostructures. Depending on the type of the nanostructures, the resultant anodes could better accommodate the large stress and strain without cracking, reduce the electronic and ionic transport pathways, and provide additional Li-storage sites.[3,105–107] The second approach is to introduce a second component to form nanocomposites; for example, metal nanoparticles can be coated with carbon or dispersed in a carbon matrix.[3,44,45,105–107] In this approach, the carbon matrix acts as a buffer for the volume change and improves the electric conductivity of the electrode. In addition, carbon phase has the advantages of low volume expansion, good ionic conductivity, and excellent tolerance to mechanical stress. The presence of carbon component can also suppress the formation of SEI film and provide additional capacity since carbon is an electrochemical active material and has considerable Li-storage capacity.[3,44,45] The third approach is to form an alloy with a second phase *M*, which is an electrochemically active or inactive component. The main role of phase *M* is to absorb the massive volume change during cycling. This second phase can also enhance the electronic conductivity of the electrode.[110–112] If the second phase *M* is electrochemically active, an intermetallic M_1–M_2, such as electrochemically active-active electroplated multiphase, is formed, in which the two different phases can act as mutual buffer to each other to overcome the large volume expansion/extraction.[113–115] This section focuses on the use of elements in groups IV (Si, Ge and Sn) and V (P and Sb) since these elements provide higher theoretical capacities compared with others and they are relatively cheap and abundant.[105–107]

3.1. Group IV elements

Group IV is also commonly called the carbon group since carbon is one of the most important elements in this group. All group IV elements have four electrons in their outermost shell, and the last orbital of all these elements is the p2 orbital. As discussed before, carbon can be used as the anode material through a Li intercalation/deintercation mechanism. However, other group IV elements form alloys with Li. Among all non-carbon group IV elements, Si is probably the most studied anode material since it exhibits a low discharge potential of 0.06 V *vs.* Li/Li^+ and has the highest theoretical specific capacity of 4200 mAh g^{-1}, which is more than ten times greater than that of graphite.[116–124] However, the low Coulombic efficiency at the initial cycle and the 400% volume change during charge/discharge hindered the large-scale commercial use of Si anodes in LIBs.[125]

Using the three strategies mentioned above, nanostructured Si,[126–129] Si/carbon nanocomposites,[105,130–137] and Si-metal alloys[138–141] have been prepared to improve the cyclability of Si-based anodes by enhancing the structural stability of Si. For example, Cho *et al.* prepared mesoporous Si/carbon core/shell nanowires with a diameter of around 6.5 nm using a butyl-capped Si as the precursor, which was impregnated into a silica SBA-15 template for multiple times and annealed at 900 °C under vacuum. The silica template was removed using hydrofluoric acid (HF) (Fig. 4a).[142] The Si/carbon composites formed from the first impregnation showed nanorod structures with 4 nm in diameter and 20 nm in length (Fig. 4b–c). Si/carbon core-shell nanowires with mesopore channels composed of thin amorphous carbon layers and Si walls were formed from the fourth impregnation (Fig. 4d–e). These as-prepared Si/carbon core/shell nanowires exhibited a high charge capacity of 3163 mAh g^{-1} (based on the total weight of Si and carbon) with a Coulombic efficiency of 86% during the first cycle at 0.2 C. After 80 cycles, the capacity was 2738 mAh g^{-1}, corresponding to a capacity retention of 87% (Fig. 4f). These mesoporous Si/carbon nanowires also showed good rate capability where the charge capacities at 0.5, 1, and 2 C were 2954, 2757, and 2462 mAh g^{-1}, respectively (Fig. 4g). The excellent electrochemical performance was attributed to the presence of ordered internal pores that were flooded with electrolyte, which ensured a high surface contact area with the electrode and hence a high flux of Li ions across the interface. In addition, the thin Si walls ensured effective diffusion pathways and high transport rates for Li ions and electrons throughout the material. Finally, both Si and carbon in the nanowires are Li-active materials and can contribute to the overall reversible capacities.

More recently, the preparation of Si/carbon composite nanofibers by embedding Si nanoparticles as an alloying medium in electrospun CNFs was reported by Zhang's group.[143–145] Anodes made from these Si/carbon composite nanofibers combined the advantages of both carbon (long cycle life and good Li-storage capacity) and Si (high Li-storage capacity) and exhibited good electrochemical performance in terms of relatively large reversible capacity (*e.g.*, around 800 mAh g^{-1} at 100 mA g^{-1}) and relatively good capacity retention (*e.g.*, 84.5% after 20 cycles) (Fig. 5). The electrospinning and subsequent carbonization are an effective method to prepare Si/carbon composite nanofibers due to the simplicity, low cost, and easy scale-up of the process.

In addition to Si, Ge and Sn are also important group IV elements that have gained attention as promising anode materials. Ge and Sn have relatively high capacities of 1600 and 992 mAh g^{-1}, respectively.[146–150] Like Si, anodes based on Ge and Sn also suffer from poor cycling performance because of the high volume changes caused by Li alloying/dealloying.[151–157] The three approaches that are used to improve Si anode performance have also been adopted to improve the cycling performance of Ge and Sn anodes.[158,159] For example, Cui *et al.* prepared Ge/carbon composite nanospheres with Ge nanoparticles dispersed in carbon matrix by the solid-state pyrolysis of tetraallylgermane.[160] These Ge/carbon nanospheres had an average diameter of 62 nm and the Ge nanoparticles encapsulated were 5 to 20 nm in size (Fig. 6a and b). These materials exhibited a highly stable and reversible capacity of 900 mA h g^{-1} after 50 cycles at 150 mA g^{-1} (Fig. 6c). At a further increase in current density from 150 to 300, 600, and 900 mA g^{-1}, highly-stable reversible capacities of approximately 774, 650, and 613 mA h g^{-1} were observed (Fig. 6d), indicating an excellent rate performance. The high performance of Li storage was ascribed to the unique nanostructure of Ge/carbon nanocomposites. The small grain size of the Ge phase reduces the Li diffusion length to a few nanometres. Nanosized carbons are Li-active and can also keep a good

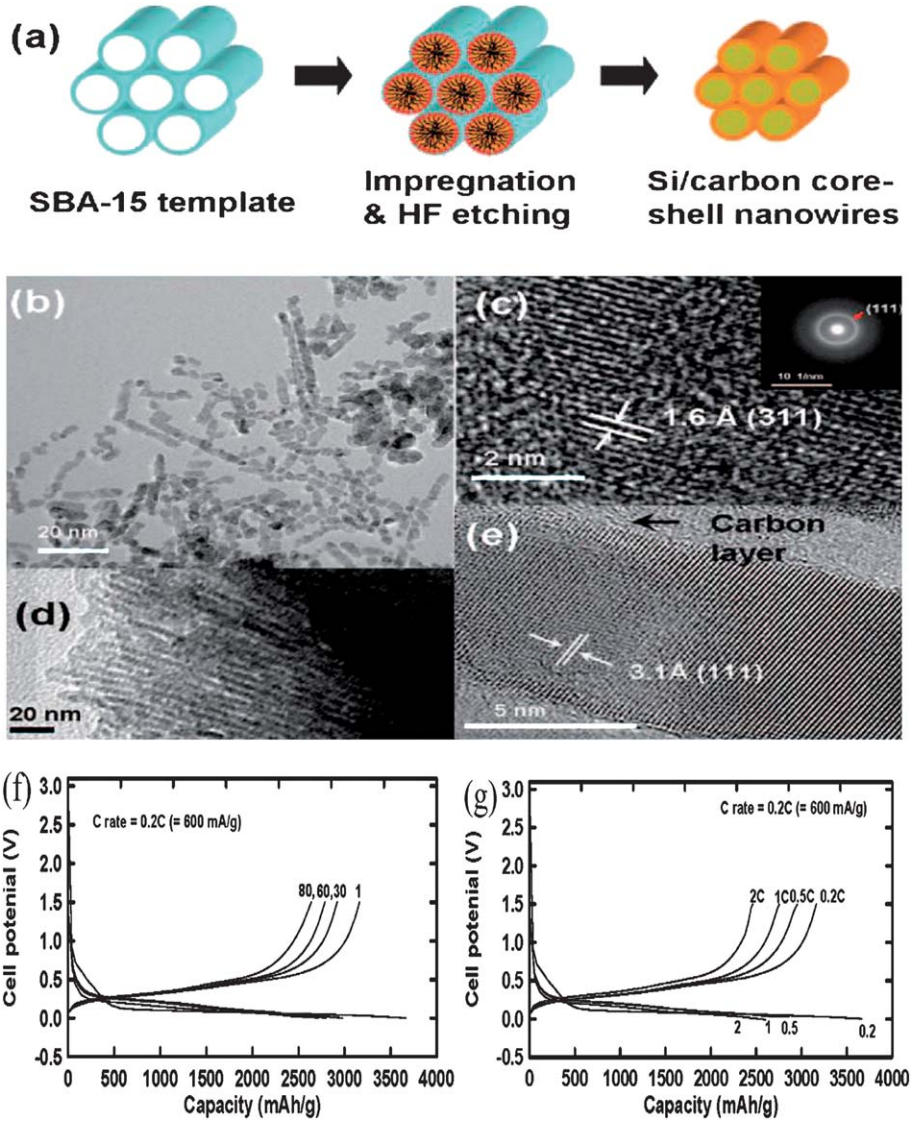

Fig. 4 (a) Schematic view of the preparation of Si/carbon core/shell nanowires. (b) TEM image of the Si/carbon core/shell nanorods obtained from first impregnation. (c) Expanded TEM image of (b). (d) TEM image of the Si/carbon core/shell nanowires obtained from fourth impregnation. (e) Expanded TEM image of (d). (f) Voltage profiles of the Si/carbon core/shell nanowires at 0.2 C. (g) Voltage profiles of the Si/carbon core–shell nanowires at 0.2, 0.5, 1, and 2 C. Reproduced with permission.[142]

electrical contact with the current collector and avoid severe agglomeration of the Ge phase. Further improvement in the electrochemical performance of Ge/carbon nanocomposites was reported by the same group where carbon was replaced by CNTs through a pyrolysis technique.[161]

Although nanostructured group IV elements and their composites have improved electrochemical performance, several problems need to be addressed, including high production cost, low tap density associated with large surface-to-volume ratio, high surface reactivity, and safety hazard associated with the flammable or explosive tendency of nanopowders.[105–107,162,182]

3.2. Group V elements

Group V elements are also called nitrogen group elements, and they have five electrons in their outermost shell. Group V element P-based nanocomposites and intermetallics (MP_n) can be used as anodes for LIBs. The high degree of electron delocalization in MP_n leads to a low oxidation state of the metal and also to a strong covalent character of M-P bond.[3,106,163] As a result, MP_n shows an overall lower insertion potential compared to the counterpart oxides. Therefore, anodes made from MP_n with small particle size can deliver large reversible capacity and good high-rate cycling stability.[164–166] MP_n can be categorized into two groups depending on the nature of the transition metal and phosphor bonding stability upon Li insertion/extraction.[106,167] The first group includes MnP_4,[163] VP_x (x = 1, 2, or 4),[168] FeP_2,[169] ZnP_2,[170] Zn_3P_2,[171,172] and NiP_2,[173,174] which realize topotactic Li insertion/extraction without breaking bonds between transition metal and phosphor. The overall reaction can be written as:[106]

$$xLi^+ + MP_n + xe^- \leftrightarrow Li_xMP_n \quad (3)$$

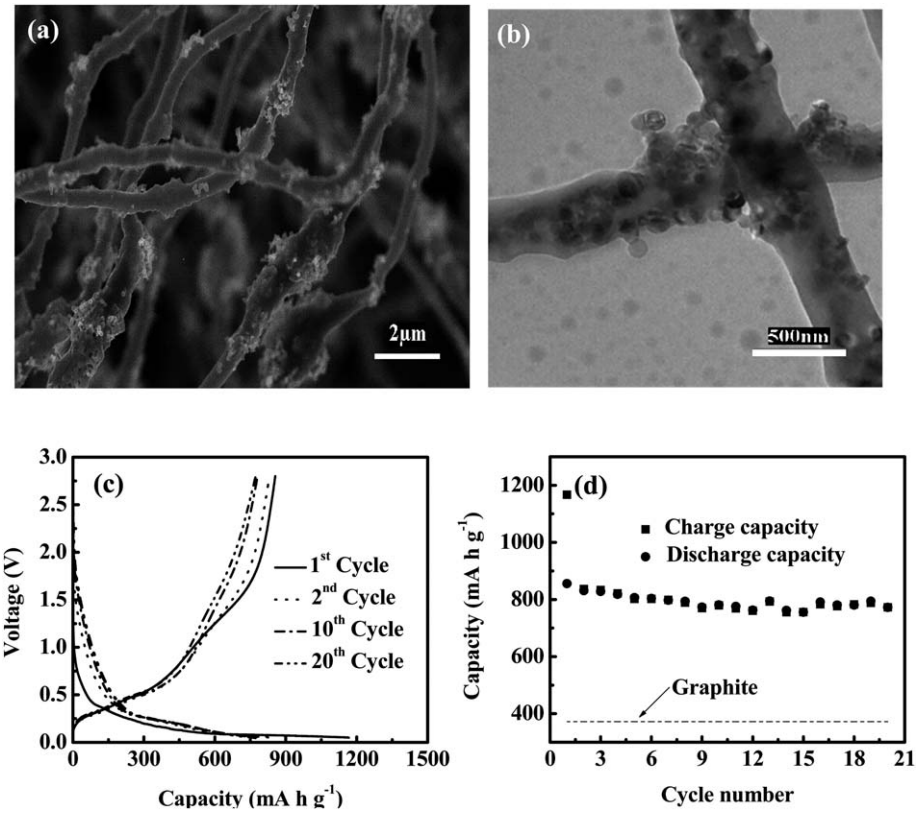

Fig. 5 (a) SEM and (b) TEM images of Si/carbon composite nanofibers, and (c) Galvanostatic charge-discharge curves and (d) cycling performance of Si/carbon nanofibers. Current density: 100 mA g^{-1}. Reproduced with permission.[143]

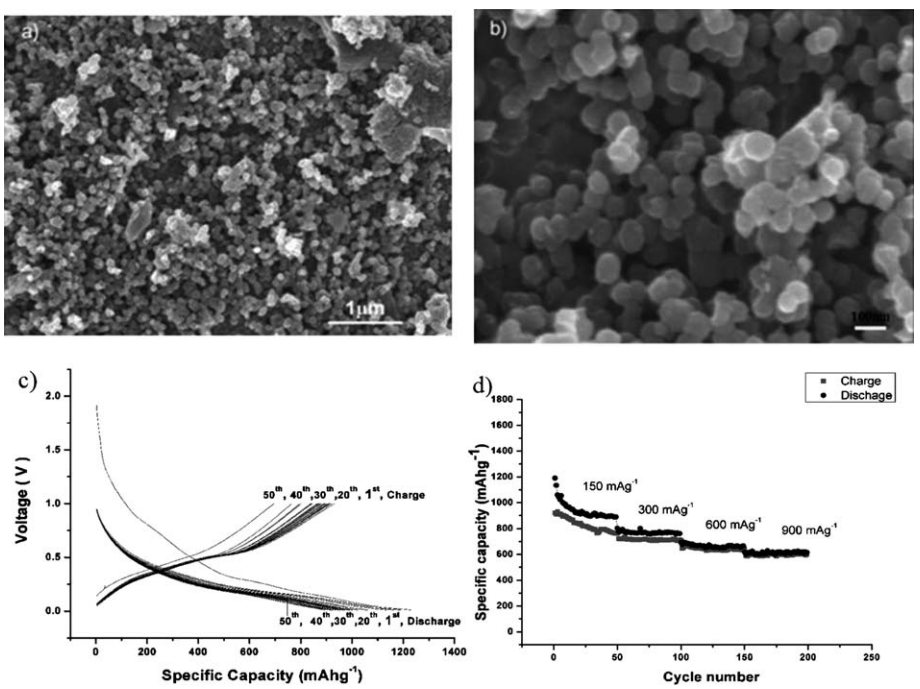

Fig. 6 (a) SEM image and (b) enlarged image of Ge/carbon nanospheres. (c) Galvanostatic charge/discharge curves of Ge/carbon nanospheres at 150 mA g^{-1}. (d) Cycling and rate performance of Ge/carbon nanospheres. Reproduced with permission.[160]

In the second group, which includes Cu_3P,[175,176] CoP_3,[177–179] Sn_3P_4,[180] NiP_2,[173] and GaP,[172] the reaction between Li and MP_n results in the direct decomposition of metal phosphide into nanosized metallic particles and Li phosphide, indicating a conversion mechanism. The reaction can be written as:[106]

$$3nLi^+ + MP_n + 3ne^- \leftrightarrow nLi_3P + M \quad (4)$$

The reversible interconversion of the crystalline phase is effected by the electrochemical redox reactions. In insertion mechanism, during the reduction (insertion) reaction, the P–P bonds in the MP_n structure are broken and form Li_xMP_n, which is reoxidated to MP_n in the reverse process. The formation of Li_xMP_n by the insertion reaction results in a stable crystalline structure with good electrochemical properties. This insertion reaction mechanism is transformed to conversion reaction during continuous charge/discharge process. The conversion reaction mechanism involves staggering uptakes of Li before the decomposed metal starts precipitating out with small structural stress. The high specific capacities of these transition metal phosphides (*e.g.*, > 1400 mAh g^{-1} for MnP_4, > 1800 mAh g^{-1} for CoP_3, > 1475 mAh g^{-1} for NiP_3) make them attractive anode candidates. However, they usually have low electrical conductivity and relatively high reaction potential. The use of these P-based anodes requires further exploration to overcome these disadvantages.[106,181]

Except for P, Group V element Sb is an attractive anode material with a high theoretical capacity of about 660 mAh g^{-1}.[106] Similarly, Sb/carbon nanocomposites and Sb-based intermetallics, especially binary compounds with other metals, have been prepared to evaluate their electrochemical performance as anodes in LIBs. Among these materials are Sb/CNT,[182] Sb/graphite,[183] Sb/polyacrylonitrile (PAN),[184] and others.[185] Similar to MP_n systems, Sb-based intermetallics and their nanocomposites are based on either insertion or conversion reaction mechanism. The materials based on the insertion reaction mechanism include Cu_2Sb,[115] ZnSb,[111] MnSb,[186] $FeSb_2$,[187] AlSb,[188] InSb,[189] and Mg_3Sb_2[190] while those based on the conversion reaction mechanism are SnSb,[154] $CoSb_3$,[191] CrSb,[192] VSb_2,[193] and $NiSb_2$.[194] High capacities were achieved for both the insertion (*e.g.*, 600 mAh g^{-1} for ZnSb/C) and conversion (*e.g.*, 700 mAh g^{-1} for SnSb/C) reactions of Sb-based nanomaterials.[105] The insertion reaction mechanism shows good initial electrochemical performance; however, it is often followed by a structural collapse during Li insertion, resulting in the transformation to a conversion reaction. The conversion reaction mechanism has reduced structural stress and this leads to a stable crystalline structure during electrochemical cycling.

Although anodes made from group V elements have shown promising properties, they still do not meet the requirements of many practical applications such as hybrid electric vehicles and advanced electrical storage devices. This is because of their expensive production cost and relatively poor capacity retention. In order to meet the requirements of commercial utilizations, a proper production process with the use of relatively cheap materials and suitable electrode designs in term of microstructures and compositions, are necessary to lower the production cost, and improve the structural stability, capacity retention, and rate capability.[106,181]

4. Metal oxides

Various metal oxides have been extensively investigated as potential anode materials for rechargeable LIBs because these materials have diverse chemical and physical properties and can deliver high reversible capacities between 500 and 1000 mAh g^{-1}.[106,181,195–201] Metal oxide-based anodes can be classified into three groups depending on their reaction mechanisms: (i) Li-alloy reaction mechanism, (ii) insertion/extraction reaction mechanism that involves the insertion and extraction of Li into and from the lattice of the transition metal oxide, and (iii) conversion reaction mechanism that involves the formation and decomposition of Li oxide (Li_2O), accompanying the reduction and oxidation of metal nanoparticles.[106,181,195–201] The three reaction mechanisms are displayed as follows:

Li-alloy reaction mechanism:

$$M_xO_y + 2yLi^+ + 2ye^- \rightarrow xM + yLi_2O \quad (5)$$

$$M + zLi^+ + ze^- \leftrightarrow Li_zM \quad (6)$$

Insertion reaction mechanism:

$$MO_x + yLi^+ + ye^- \leftrightarrow Li_yMO_x \quad (7)$$

Conversion reaction mechanism:

$$M_xO_y + 2yLi^+ + 2ye^- \leftrightarrow xM + yLi_2O \quad (8)$$

4.1. Li-alloy reaction mechanism

SnO_2 is the most important metal oxide in this category. On the first charge, Li bonds to the oxygen in SnO_2 forming Li_2O and Sn, and the latter continues to form alloy with Li with an upper-limit of $Li_{4.4}Sn$, corresponding to a theoretical capacity of 783 mAh g^{-1}.[202–205] However, upon continuous cycling, Sn phases produced from the delithiation of the Li–Sn alloy showed a tendency to aggregate with each other and form clusters. This causes fast deterioration in the reversible capacity because of the volume change of Sn and the destruction of Li_2O matrix that hold reduced Sn particles upon Li insertion.[106,206,207] Much attention has been paid to improve the cycling performance of SnO_2 and reduce the irreversible capacity. Porous SnO_2 nanostructure, SnO_2-based nanocomposites,[208–210] nanostructured SnO_2 thin films[211] and hollow core-shell mesospheres[212] are representative material systems developed in this direction.

Compared with solid SnO_2 particles, porous SnO_2 nanostructures can suppress volume changes since the pores act as the structure buffer for the large volume changes during cycling.[213] Using silica as template, Cho *et al.* prepared mesoporous SnO_2-based anodes that delivered a reversible capacity of 800 mAh g^{-1} at 0.2 C with a capacity retention of 98% after 50 cycles.[214] Hyeon *et al.* also synthesized porous SnO_2 microspheres using $SnCl_4 \cdot 5H_2O$ and resorcinol-formaldehyde gel.[215] The resultant anodes delivered a discharge capacity of 952 mAh g^{-1}. However, the major drawback of these porous SnO_2 materials is the large irreversible capacities caused by their large surface areas.

SnO_2/carbon nanostructured composites, such as SnO_2/carbon nanocolloids,[216] SnO_2/carbon nanoparticles,[217] SnO_2/CNTs,[218] SnO_2/carbon hollow nanospheres,[219] and porous SnO_2 nanotubes with coaxially grown CNT overlayers,[220] were also prepared. The results showed most of these materials had high reversible Li storage capacities and improved cycling performance. This stems from the synergistical combination of the good stability of conductive carbon matrices and high Li-storage capacity of SnO_2 nanoparticles. For these SnO_2/carbon nanocomposites, carbon acts as a barrier to prevent the aggregation between SnO_2 particles by providing a buffering space where SnO_2 particles can experience the volume change without collapsing. Furthermore, carbon itself is an active material for additional Li storage. Recently, Zhang's group prepared carbon-SnO_2 core-sheath composite nanofibers using electrospinning and electrodeposition strategies.[221] The as-prepared core-sheath composite nanofibers were used as binder-free anodes and delivered a discharge capacity of around 800 mAh g^{-1} at the first cycle at 50 mA g^{-1}, with 69% capacity retention after 100 cycles. These anodes can withstand large volume expansion and contraction during Li insertion/extraction because the carbon fiber cores act as efficient electron transport pathways and stable mechanical support for keeping the structural integrity of the electrodes during cycling.

4.2. Insertion reaction mechanism

Several transitional metal oxides can store Li *via* the insertion reaction mechanism.[106] These materials are attractive anode materials for rechargeable LIBs due to their low cost and non-toxicity. However, the number of electrons involved in the insertion reaction is generally less than one per Li because Li can only be accommodated into the vacant sites of the frameworks in these metal oxides. Therefore, insertion reaction-based metal oxide anodes have relatively low specific capacity.[222–224] For example, TiO_2 has various polymorphs such as anatase, rutile, and TiO_2–B. Anatase is generally considered the most electroactive Li-insertion host, because anatase TiO_2 is not only a low voltage insertion host for Li but also has fast Li insertion/extraction kinetics.[222–224] Guo *et al.* recently prepared nanostructured mesoporous anatase TiO_2 that exhibited high Li-storage capacity and excellent cycling performance.[222–224] TiO_2 nanowires and nanotubes are also attractive anode materials. Results reported by Zhou *et al.* on TiO_2 nanotubes with mesoporous walls within anodic aluminium oxide membranes showed a Li-storage capacity of 340 mAh cm^{-3}. The nanotube structure of these TiO_2 provided effective pathways for both Li ions and electrons which are essential for high-rate rechargeable LIBs.[87,225] WO_2 is another transitional metal oxide with Li insertion storage mechanism, which demonstrates a low working potential; however, this material usually undergoes severe irreversible decomposition and shows poor cycle performance.[226,227]

4.3. Conversion reaction mechanism

The conversion reaction mechanism has brought great interest since many important transitional metal oxides (MO_x, where M = Fe, Co, Ni, Cu, Mo, Ni, Gr, Ru, *etc.*) follow that mechanism during electrode reactions.[106,181,209] According to eqn (8), these oxides are converted to a metallic state along with Li_2O component at the first lithiation and are reversibly returned to its initial state after delithiation. Anodes made from these metal oxides exhibit high reversible capacities and high energy densities because the oxidation state is utilized fully and more than one electron are involved in the conversion reaction.[106,181,187,203,228] However, they often show low Coulombic efficiency at the first cycle, unstable SEI film formation, large potential hysteresis, and poor capacity retention. To solve these problems, nanostructured porous transition metal oxide materials and transition metal oxide/carbon nanocomposites have been prepared.[38–46,106,181,207–209] In the following section, we discuss the most widely studied conversion reaction-based transition metal oxide anodes, *i.e.*, iron oxides, cobalt oxides, manganese oxides, molybdenum oxides, and copper oxides, as shown in Table 1. Moreover, other transition metal oxide anodes and their representative nanostructures, *i.e.*, chromium oxides, nickel oxides, and ruthium oxides, have also been summarized in Table 1.

4.3.1. Iron oxides. Iron oxides, such as hematite (Fe_2O_3) and magnetite (Fe_3O_4), are attractive conversion reaction-based anode materials for rechargeable LIBs because of their low cost and non-toxicity.[203,228] Li can be reversibly inserted into Fe_2O_3 in a wide potential range, *e.g.*, 1.5–4.0 V *vs.* Li/Li^+. When lowering the potential to 0.9 V, additional two moles of Li can be inserted but they cannot be extracted without damaging the crystal structure of the material.[229,230] After discharging to 0.005 V, 8.5 moles of Li can be further inserted. This yields a total theoretical capacity of 1007 mAh g^{-1} by the formation of Fe^0 from Fe^{3+}. Studies by Larcher *et al.*[229] and Morales *et al.*[231] on Fe_2O_3 nanoparticles and by Chen *et al.*[232] on Fe_2O_3 nanotubes indicated that the morphology of nanosized Fe_2O_3 structures plays a significant role in the reactivity towards Li, and demonstrated that four moles of Li are cyclable in the potential range of 0.005–3.0 V. However, severe capacity degradation occurred during the long-term cycling. Zhang *et al.* fabricated fiber-like Fe_2O_3 macroporous nanomaterials by the *in situ* synthesis of Fe_2O_3 in regenerated cellulose fibers, followed by the removal of cellulose matrix *via* calcination.[233] These Fe_2O_3 nanomaterials presented a large discharge capacity of 2750 mAh g^{-1} at the first cycle and 732 mAh g^{-1} after 50 cycles. This large discharge capacity might be due to both the increased surface area of Fe_2O_3 and the carbon remained after calcination, which contributes to additional Li storage, as well as their special nanotructures.[234,235,236]

In addition to Fe_2O_3, Fe_3O_4 is also a promising high-capacity anode material that can deliver a theoretical capacity up to 926 mAh g^{-1}.[237,238] Zhang *et al.* synthesized carbon-coated Fe_3O_4 nanospindles by partial reduction of monodispersed Fe_2O_3 nanospindles with carbon coatings.[237] SEM images on the Fe_3O_4 nanospindles showed that these spindle-like nanostructures were composed of tiny crystals with an average length of 470 nm and a diameter of 106 nm (Fig. 7a-b). After a heat-treatment at 600 °C, Fe_3O_4-carbon spindles of 428 nm in length and 100 nm in diameter with small void space at the tips were obtained (Fig. 7c). The TEM image in Fig. 7d showed that the carbon layer had a uniform and continuous structure with a thickness of 2–10 nm. At the first cycle, the carbon-coated Fe_3O_4 nanospindles showed a high reversible capacity of 745 mAh g^{-1} at C/5. The capacity remained almost unchanged after four subsequent cycles.

Table 1 Summarization of conversion reaction-based nanotructured transitional metal oxide anodes

Metal oxides		Theoretical capacities (mAh g^{-1})	Representive nanostructures	Common problems and possible solutions
Iron oxides	Fe_2O_3	1007[229,230]	Nanostructures and carbon-based nanocomposites[231–237]	Common problems: Low Coulombic efficiency at the first cycle, unstable SEI film formation, large potential hysteresis, and poor capacity retention.
	Fe_3O_4	926[231–238]		
Cobalt oxides	Co_3O_4	890[86]	Nanostructured Co_3O_4 or Co_3O_4/carbon nanocomposites[240–246]	
	CoO	715[239]	CoO composites[247–250]	
Manganese oxides	MnOx	700–1000[260,261]	Nanostructures[256,262,264] MnOx/carbon[266,267]	Possible solutions: 1. Metal oxide/carbon composites using carbon as buffer and electrode-active materials. 2. Nanostructured metal oxides to provide high surface area and quantum confinement effects.
Molybdenum oxides	MoO_3	1111[269,270]	Doped MoO_3[271–275]	
	MoO_2	830[269,270]	MoO_2 nanomaterials[276]	
Copper oxides	CuO	674[284,285]	Nanostructured CuO[278,279,283–291]	
	Cu_2O	375[293]	Cu_2O/Carbon composites[294–298]	
Chromium oxides	Cr_2O_3	1058[299]	Nanostructures, hetero-atom doping, and carbon-based nanocomposites[300–302]	
Nickel oxides	NiO	718[203]	NiO/carbon[303] Porous NiO[304]	
Ruthenium oxides	RuO_2	1130[305]	SnO_2/RuO_2[306,307]	

Compared with bare Fe_3O_4 spheres, these carbon-coated Fe_3O_4 nanospindles showed higher Coulombic efficiency and better cycling performance (Fig. 7e–f). Zhang *et al.* attributed these improvements to the uniform and continuous carbon coating layers, which helped to maintain the integrity of spindles and increased the electronic conductivity of the electrodes.[237] More work is needed to completely understand this performance improvement mechanism.

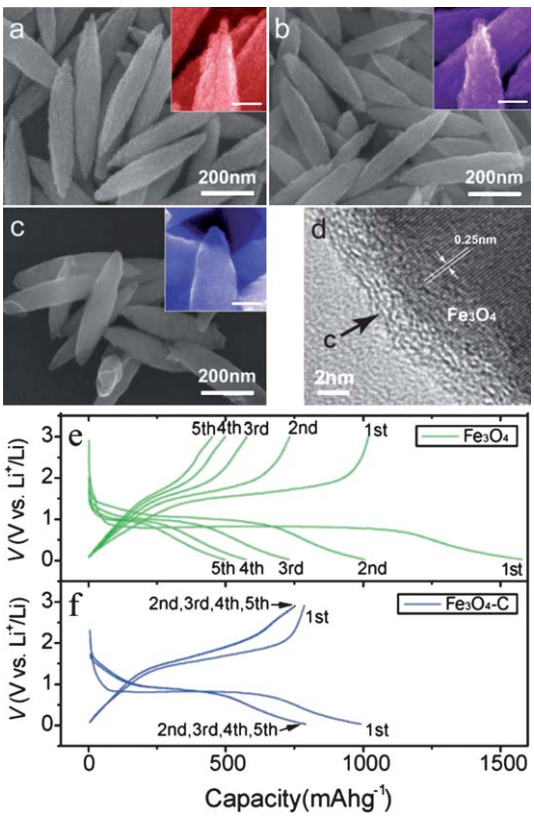

Fig. 7 SEM images of (a) as-synthesized Fe_2O_3 spindles, (b) carbon precursor-coated Fe_2O_3 spindles, and (c) carbon-coated Fe_3O_4 spindles. (d) TEM image of carbon-coated Fe_3O_4 spindles. The insets are close views of corresponding samples, all unmarked scale bars are 50 nm. The discharge/charge profiles of (e) commercial Fe_3O_4 particles and (f) carbon-coated Fe_3O_4 spindles at C/5. Reproduced with permission.[237]

4.3.2. Cobalt oxides. Cobalt oxides such as Co_3O_4 and CoO have relatively high theoretical capacities of 890 and 715 mAh g^{-1}, respectively.[86,239] Recently, Co_3O_4-based nanomaterials were synthesized to be used as LIB anodes, including mesoporous Co_3O_4,[240] porous Co_3O_4 nanosheets,[241] Co_3O_4 nanowire arrays,[240,242] needle-like Co_3O_4 nanotubes,[243] multiwalled CNT/Co_3O_4 nanocomposites,[244,245] and Co_3O_4 nanorods.[246] Li *et al.* developed a template-free method for the large-area growth of self-supported Co_3O_4 nanowire arrays.[242] The nanowires were 500 nm in diameter and 15 μm in length and they grew almost vertically from the substrate (Fig. 8a–b). The Co_3O_4 nanowire arrays showed superior capacity retention compared to other unsupported nanowires and commercial powders. Results reported on the self-supported Co_3O_4 nanowire arrays showed large charge and discharge capacities of approximately 1124 and 859 mAh g^{-1}, respectively, at the first cycle at 1 C. The nanowire arrays maintained a stable capacity of 700 mAh g^{-1} after 20 cycles. Under the same conditions, commercial Co_3O_4 powders gave a significantly lower capacity of 80 mAh g^{-1} and unsupported nanowires only showed a moderate capacity of 350 mAh g^{-1} after 20 cycles (Fig. 8c). The self-supported Co_3O_4 nanowire arrays also showed high rate capability (Fig. 8d). The large capacity and high rate capability of self-supported nanowire arrays result from their unique hierarchical architecture. CoO nanostructured materials, such as Li_2O–NiO–CoO composites[247] and Ni-foam-supported reticular CoO–Li_2O composites,[248] have also been studied for use as anodes for LIBs. Xia *et al.* prepared CoO nanoparticle-loaded hollow carbon spheres by a wet-penetration method.[249] The hollow carbon spheres played the role of structural support, which hampered CoO particles from agglomeration as well as acted as a host for Li storage. Zhang

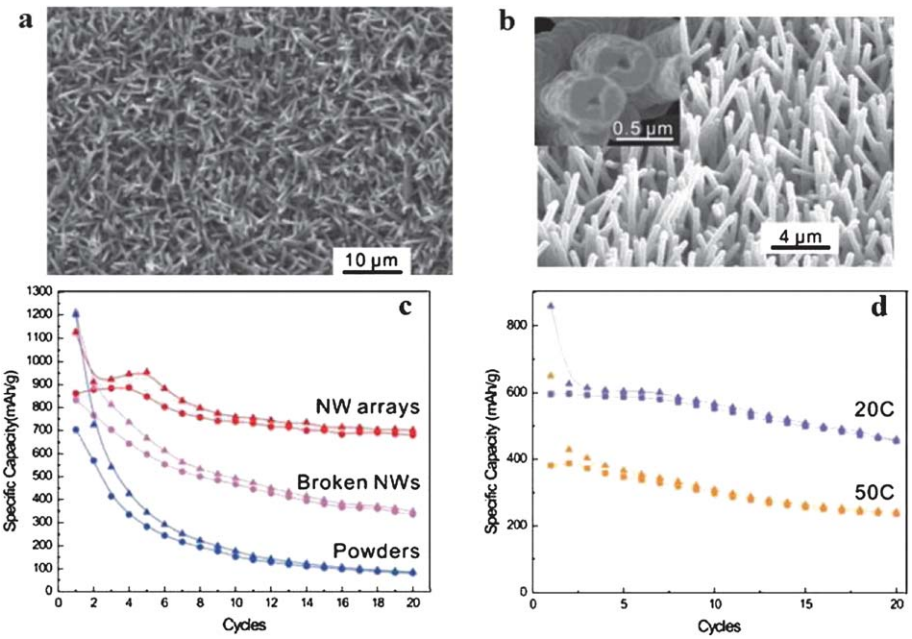

Fig. 8 SEM images of Co_3O_4 nanowire arrays grown on Ti foil viewed from (a) the top and (b) when tilted by 40°. The inset of (b) shows the open tips of the nanowires. (c) Specific capacity of self-supported Co_3O_4 nanowire arrays, unsupported (broken) Co_3O_4 nanowires, and commercial Co_3O_4 powders as a function of cycle number. For each set of data, the upper curve is for discharge and the lower curve is for charge. (d) Specific capacity of the Co_3O_4 nanowire arrays at 20 and 50 C as a function of cycle number. Reproduced with permission.[242]

et al. also improved the performance by synthesizing CoO/carbon hybrid microspheres *via* a solvothermal approach.[250]

4.3.3. Manganese oxides. Manganese oxides, such as Mn_2O_3,[251,252] Mn_3O_4,[253,254] and MnO,[255–257] can also be used as anodes.[181,258,259] The theoretical capacities of manganese oxides as anode materials are between 700–1000 mAh g^{-1} depending on their chemical and physical structures.[260,261] The application of manganese oxide-based anodes in practical LIBs is challenging because of their poor electrical conductivity and large volume change during cycling. A promising method to alleviate these problems is to use nanostructured manganese oxide-based anodes, such as MnO[256] nanocrystalline, MnO thin films,[262] Mn_3O_4 nanofibers,[263] and interconnected MnO_x nanowires.[199,264] The limited substitution of Mn by Co or Zn in Mn_3O_4 materials can also improve their electrochemical performance.[254,265] Recently, the synthesis of porous manganese oxide/carbon composite nanofibers by electrospinning PAN/$Mn(CH_3COO)_2$ precursor followed by a thermal treatment process was reported by Zhang's group.[266,267] As seen in Fig. 9a-b, the SEM and TEM images showed that MnO_x/carbon nanofibers had uneven convolute and undulated surface morphology with a large variation in fiber diameters. The charge and discharge capacities of these composite fibers were 1155 and 785 mAh g^{-1}, respectively, at 50 mA g^{-1} at the first cycle.[266,267] A highly stable and reversible capacity of 600 mAh g^{-1} was achieved at the 50th cycle, which was 76% of the initial reversible capacity (Fig. 9c). These porous MnO_x/carbon nanofiber anodes were cycled at higher current densities and showed a relatively good rate capability (Fig. 9d).[266,267] More recently, the same group also prepared MnO_x/carbon nanofiber composites through electrodepositing MnO_x nanoparticles onto electrospun CNFs.[268] These nanocomposites exhibited a stable reversible capacity of approximately 500 mAh g^{-1} after 50 cycles at 50 mA g^{-1}. At high current density of 500 mA g^{-1}, a stable reversible capacity of 400 mAh g^{-1} was also obtained.[268]

4.3.4. Molybdenum oxides. MoO_3 and MoO_2 can also store Li through the conversion reaction and can deliver high theoretical specific capacities of 1111 mAh g^{-1} and 830 mAh g^{-1}, respectively.[269,270] MoO_3 is often doped with Na and Sn to improve the capacity retention and rate capability.[271,272] The electrochemical performance was further improved by using MoO_3- and MoO_2-based nanostructures,[273,274] and nanocomposites.[275] Recently, Shi *et al.* synthesized a highly-ordered mesoporous crystalline MoO_2 *via* a nanocasting strategy.[276] This material showed a typical metallic conductivity and exhibited improved charge/discharge capacities and enhanced cycle life, because the material partially lost its crystallinity and transformed to an amorphous-like structure during cycling. The improved Li diffusion kinetics and the reversible formation/decomposition of the SEI film may also play an important role.[277]

4.3.5. Copper oxides. CuO[203,278,279] and Cu_2O[203,280] are well-known p-type semiconductors and can be attractive anode materials for rechargeable LIBs due to their nontoxic nature and affordable price. Pure CuO and Cu_2O anodes also suffer from large volume change during cycling. To reduce the volume change and improve the cycle life of these anodes, nanostructured copper oxides[2,3,96] and nanocomposites[281] were prepared.

The reversible capacity of CuO is closely related to the product formed during the discharging process. Results reported by

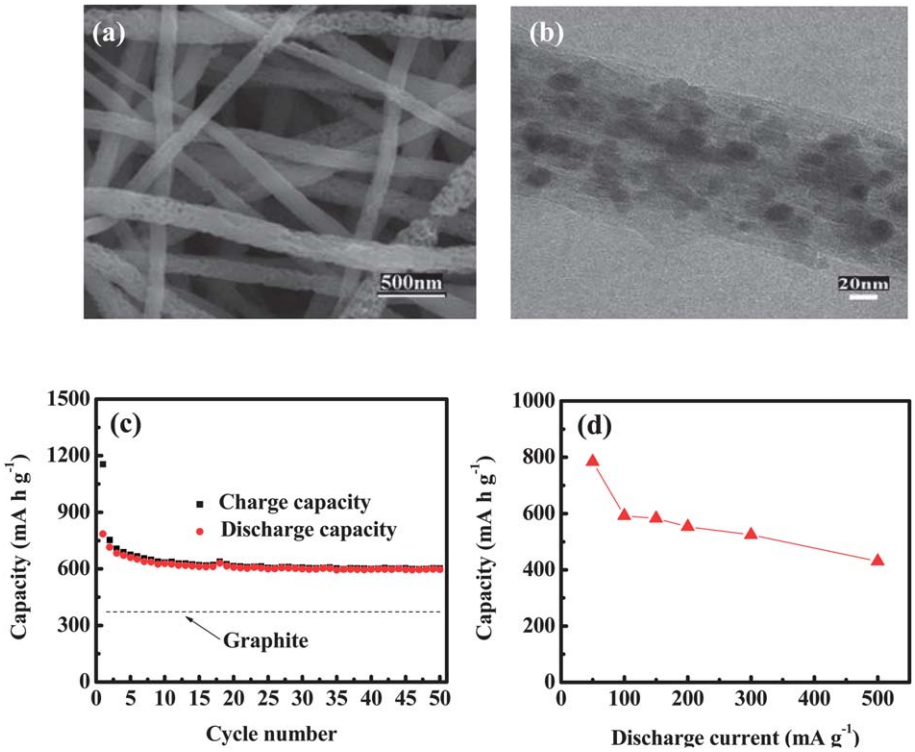

Fig. 9 (a) SEM and (b) TEM images of porous MnO_x/carbon nanofibers, (c) cycling performance at 50 mA g^{-1}, and (d) reversible capacity *vs.* current density for porous MnO_x/carbon nanofibers. Reproduced with permission.[267]

Tarascon *et al.* showed that CuO was reduced to Cu nanograins during the charge process through an intermediate Cu_2O phase.[282,283] However, the reduced metallic Cu re-oxidized back to Cu_2O instead of CuO during discharge. The charge/discharge mechanism was observed and confirmed by several other groups.[284,285] Wu *et al.* prepared hierarchical CuO spheres with radiating nanoplates[285] and a charge capacity of 800 mAh g^{-1} and a discharge capacity of approximately 250 mAh g^{-1} at the first cycle were observed. These values indicated that the reduced metallic Cu can only be re-oxidized to Cu_2O.[285] A theoretical capacity of 674 mAh g^{-1} can be obtained if the reduced metallic Cu can be re-oxidized back to CuO. CuO nanomaterial anodes, such as CuO nanoribbon arrays,[286] CuO nanowires,[287] CuO nanorods,[288] and nanoflower-like CuO/Ni films,[289] CuO/graphite composites,[290] and CuO/CNT composites[291] were also reported.

Cu_2O is nontoxic and abundant in nature.[292,293] Results from charge-discharge and cyclic voltammetry experiments revealed that the morphology and crystallinity of Cu_2O play important roles in determining the electrochemical performance. Cu_2O nanostructures, such as Cu_2O nanorod arrays,[294] Cu_2O nanoparticles,[295] and Cu_2O nanofilms,[296] and Cu_2O-based nanocomposites, such as Cu_2O/graphite,[280] core–shell Cu_2O/Cu,[292] Cu_2O–Li_2O,[297] and porous Cu_2O/CuO nanocomposites,[298] were synthesized and used as anodes for LIBs.

5. Metal sulfides/nitrides

A variety of transition metal-containing sulfides MS_2 (M = Fe, Ti, Co, Ni, and Cu) have been studied as cathode materials.[308–310] In contrast, many other layered metal sulfides MS_2 (M = Mo, W, Ga, Nb, and Ta) can be used as anode materials because they act as host lattices when reacting with a variety of guest atoms or molecules to yield intercalation compounds. Layered metal sulfides have a similar structure to graphitic carbon and can form inorganic fullerene-like structures. A key feature of these sulfides is the existence of Van der Waals force across gaps between S–M–S sheets, which provide space for guest reactants. During Li intercalation, a complete charge transfer occurs, which involves not only the reduction of M^{4+} to M^{3+} but also the diffusion of Li ions into the Van der Waals gaps.[311,312] Anodes made from these layered transition metal sulfides show reasonable capacity and good cycling stability. Wang *et al.* found that Li could be intercalated into WS_2 nanotubes.[313] The results showed a capacity of 350 mAh g^{-1} at a cut-off voltage window of 0.1–1.5 V *vs.* Li/Li^+. In addition, a capacity of 790 mAh g^{-1} in a voltage range of 0.01–3.0 V *vs.* Li/Li^+ was observed on WS_2 nanoflakes, and this corresponds to 7.4 mol Li per mole of WS_2.[311] The high capacity was attributed to the intercalation of Li into intratubular and intertubular sites of WS_2 nanotubes as well as the diffusion into the WS_2 structure to form Li_xWS_2 intercalation compounds. However, since Li can intercalate into small holes/channels, defects in WS_2 nanotubes and a relatively large volume change during cycling can result in structural instability and poor cycling performance. Except for the layered transitional metal sulfides, many other metal sulfides such as Co_9S_8,[314] ZnS,[315] Li_2SiS_3,[316] and Al_2S_3,[317] were also reported to react with Li following a conversion reaction mechanism to produce Li_2S and metal nanoparticles when used as LIB anodes.[181]

Li transition metal nitrides have also emerged as promising anode candidates for LIBs because their layered morphology can

support fast Li ion conduction and low transition metal oxidation states.[318] The first metal nitride studied was $LiMoN_2$,[319] but the materials capturing current interest are antifluorite-type Li_7MnN_4 and $Li_{7.9}MnN_{3.2}O_{1.6}$ which showed reversible capacities in excess of 300 mAh g^{-1} with excellent retention, most likely due to the small volume change during charge/discharge.[320,321] The capacity of Li metal nitrides was improved by the synthesis of $Li_{2.6}Co_{0.4}N$ to between 480 and 760 mAh g^{-1}.[322] The new compound of $Li_{2.7}Fe_{0.3}N$, with a reversible capacity of 550 mAh g^{-1}, was prepared by Rowsell *et al.* and preliminary results showed good rate capability over cycling.[318] Other metal nitrides, such as Sb_3N,[323] Zn_3N_2,[324] Ge_3N_4,[325] SnN_x,[326] and VN,[327] were also studied as anodes for LIBs *via* conversion reactions.[181]

6. Summary and outlook

As one of the most promising energy storage technologies, LIBs are dominantly powering most of today's portable electronics. However, they fall short of meeting the demands in powering advanced hybrid electric vehicles and plug-in electric vehicles because of their relatively low energy and power densities, poor durability, and high cost. Advances in nanoscience and nanotechnology have presented the opportunity to design novel energy-storage materials for the next-generation high-performance LIBs with higher capacity and longer cycle life. Due to the high surface area of nanostructured materials, these materials can provide high Li-ion flux across the interface, short diffusion pathways for both Li ions and electrons, abundant active sites for Li storage, and high freedom for volume change during charge/discharge to enhance the structural stability of the electrodes.

In this review article, four categories of LIB anode materials were discussed. The first one is nano-carbons, which can store Li through an intercalation process. The improved storage ability is closely related to their surface area, crystallinity, morphology as well as the orientation of the crystallites. In the second group, alloying materials such as groups IV and V elements were presented. These materials can electrochemically alloy with Li and provide larger specific capacities compared with carbonaceous materials. However, these materials suffer from large volume change upon Li alloying/dealloying which leads to severe capacity fading. Downsizing these bulk materials to the nanoscale, dispersing these elements into active and/or inactive matrices and preparing intermetallic alloy materials have been used to overcome the above-mentioned problems and improve the overall electrochemical performance. The third category is metal oxides which usually react with Li through alloying, insertion or conversion mechanisms. Their large-scale application is also hindered by the rapid capacity decay during charging/discharging because of the enormous volume change. Various types of metal oxide-based nanostructures and nanocomposites have been developed to address this problem. The final category is metal sulfide/nitride nanostructures which have also been demonstrated to be promising anode materials for LIBs since they can support fast Li-ion conduction and low transition metal oxidation states. However, the use of these materials as anodes for LIBs is still far from reality because of their high cost, poor safety, poor rate capability, and low capacity.

To realize wide-spread commercial applications, further work is required to achieve controlled and large-scale synthesis of nanostructures. It is also necessary to understand the mechanisms of Li storage in nanomaterials and the kinetic transport at the electrode/electrolyte interface since reactions in LIBs start at the interface between electrode and electrolyte. Further considerations include the development of predictive theoretical tools for a better fundamental understanding of the relationships between nanostructures and electrochemical characteristics of these novel nanostructured anode materials.[328–331]

The future directions of nanostructured anode materials for rechargeable LIBs should focus on exploring new types of Li-ion redox couples with different electrode reaction mechanisms and designing novel micro-structures and morphology in order to further increase battery energy/power densities, enhance charge/discharge rate capability, improve service life and safety, and reduce the cost at the same time. As the science of producing high-energy and high-power batteries matures, the preparation of nanostructured anode materials *via* more sustainable and greener strategies or from renewable resources should also be addressed to limit environment pollution and to secure a bright future for human beings and also for our world as a whole.[328–331]

Acknowledgements

We thank funding supports by the Department of Energy (NO. DE-EE0001177) and the ERC Program of the National Science Foundation Award (No. EEC-08212121). We also thank Mr Richard Padbury and Mr Yingfang Yao for helpful discussions and revisions.

References

1 J. W. Long, B. Dunn, D. R. Rolison and H. S. White, *Chem. Rev.*, 2004, **104**, 4463.
2 J. Chen and F. Y. Cheng, *Acc. Chem. Res.*, 2009, **42**, 713.
3 M. G. Kim and J. Cho, *Adv. Funct. Mater.*, 2009, **19**, 1497.
4 P. G. Bruce, B. Scrosati and J. M. Tarascon, *Angew. Chem., Int. Ed.*, 2008, **47**, 2930.
5 M. Winter and R. J. Brodd, *Chem. Rev.*, 2004, **104**, 4245.
6 A. S. Arico, P. Bruce, B. Scrosati, J. M. Tarascon and W. Van Schalkwijk, *Nat. Mater.*, 2005, **4**, 366.
7 J. Baxter, Z. X. Bian, G. Chen, D. Danielson, M. S. Dresselhaus, A. G. Fedorov, T. S. Fisher, C. W. Jones, E. Maginn, U. Kortshagen, A. Manthiram, A. Nozik, D. R. Rolison, T. Sands, L. Shi, D. Sholl and Y. Y. Wu, *Energy Environ. Sci.*, 2009, **2**, 559.
8 D. Deng, M. G. Kim, J. Y. Lee and J. Cho, *Energy Environ. Sci.*, 2009, **2**, 818.
9 K. S. Kang, Y. S. Meng, J. Breger, C. P. Grey and G. Ceder, *Science*, 2006, **311**, 977.
10 A. Manthiram, A. V. Murugan, A. Sarkar and T. Muraliganth, *Energy Environ. Sci.*, 2008, **1**, 621.
11 Y. S. Meng and M. E. Arroyo-de Dompablo, *Energy Environ. Sci.*, 2009, **2**, 589.
12 J. M. Tarascon and M. Armand, *Nature*, 2001, **414**, 359.
13 V. Thavasi, G. Singh and S. Ramakrishna, *Energy Environ. Sci.*, 2008, **1**, 205.
14 M. Wakihara, *Mater. Sci. Eng., R*, 2001, **33**, 109.
15 M. S. Whittingham, *Chem. Rev.*, 2004, **104**, 4271.
16 M. Winter, J. O. Besenhard, M. E. Spahr and P. Novak, *Adv. Mater.*, 1998, **10**, 725.
17 J. Chen, J. Z. Wang, A. I. Minett, Y. Liu, C. Lynam, H. K. Liu and G. G. Wallace, *Energy Environ. Sci.*, 2009, **2**, 393.
18 B. J. Landi, M. J. Ganter, C. D. Cress, R. A. DiLeo and R. P. Raffaelle, *Energy Environ. Sci.*, 2009, **2**, 638.
19 M. R. Palacin, *Chem. Soc. Rev.*, 2009, **38**, 2565.
20 H. Zhang, G. P. Cao and Y. S. Yang, *Energy Environ. Sci.*, 2009, **2**, 932.

21 Y. G. Guo, J. S. Hu and L. J. Wan, *Adv. Mater.*, 2008, **20**, 2878.
22 M. Armand, S. Grugeon, H. Vezin, S. Laruelle, P. Ribiere, P. Poizot and J. M. Tarascon, *Nat. Mater.*, 2009, **8**, 120.
23 J. M. Tarascon, N. Recham, M. Armand, J. N. Chotard, P. Barpanda, W. Walker and L. Dupont, *Chem. Mater.*, 2010, **22**, 724.
24 H. Li, Z. X. Wang, L. Q. Chen and X. J. Huang, *Adv. Mater.*, 2009, **21**, 4593.
25 A. K. Padhi, K. S. Nanjundaswamy and J. B. Goodenough, *J. Electrochem. Soc.*, 1997, **144**, 1188.
26 B. Peng and J. Chen, *Coord. Chem. Rev.*, 2009, **253**, 2805.
27 J. R. Dahn, T. Zheng, Y. H. Liu and J. S. Xue, *Science*, 1995, **270**, 590.
28 K. Sato, M. Noguchi, A. Demachi, N. Oki and M. Endo, *Science*, 1994, **264**, 556.
29 K. Persson, V. A. Sethuraman, L. J. Hardwick, Y. Hinuma, Y. S. Meng, A. van der Ven, V. Srinivasan, R. Kostecki and G. Ceder, *J. Phys. Chem. Lett.*, 2010, **1**, 1176.
30 B. Ellis, P. S. Herle, Y. H. Rho, L. F. Nazar, R. Dunlap, L. K. Perry and D. H. Ryan, *Faraday Discuss.*, 2007, **134**, 119.
31 A. K. Shukla and T. P. Kumar, *Curr. Sci.*, 2008, **94**, 314.
32 Y. Xie and C. Z. Wu, *Dalton Trans.*, 2007, 5235.
33 P. Balaya, *Energy Environ. Sci.*, 2008, **1**, 645.
34 C. H. Jiang, E. Hosono and H. S. Zhou, *Nano Today*, 2006, **1**, 28.
35 M. S. Park, G. X. Wang, Y. M. Kang, D. Wexler, S. X. Dou and H. K. Liu, *Angew. Chem., Int. Ed.*, 2007, **46**, 750.
36 M. S. Whittingham, *Dalton Trans.*, 2008, 5424.
37 N. H. Zhao, L. J. Fu, L. C. Yang, T. Zhang, G. J. Wang, Y. P. Wu and T. van Ree, *Pure Appl. Chem.*, 2008, **80**, 2283.
38 J. B. Goodenough and Y. Kim, *Chem. Mater.*, 2010, **22**, 587.
39 J. W. Fergus, *J. Power Sources*, 2010, **195**, 939.
40 A. Ritchie and W. Howard, *J. Power Sources*, 2006, **162**, 809.
41 M. M. Thackeray, J. T. Vaughey and L. M. L. Fransson, *JOM*, 2002, **54**, 20.
42 A. G. Ritchie, *J. Power Sources*, 2001, **96**, 1.
43 S. Flandrois and B. Simon, *Carbon*, 1999, **37**, 165.
44 N. A. Kaskhedikar and J. Maier, *Adv. Mater.*, 2009, **21**, 2664.
45 C. Liu, F. Li, L. P. Ma and H. M. Cheng, *Adv. Mater.*, 2010, **22**, E28.
46 Y. G. Wang, H. Q. Li, P. He, E. Hosono and H. S. Zhou, *Nanoscale*, 2010, **2**, 1294.
47 S. Iijima, *Nature*, 1991, **354**, 56.
48 A. C. Dillon, *Chem. Rev.*, 2010, **110**, 6856.
49 B. Gao, C. Bower, J. D. Lorentzen, L. Fleming, A. Kleinhammes, X. P. Tang, L. E. McNeil, Y. Wu and O. Zhou, *Chem. Phys. Lett.*, 2000, **327**, 69.
50 J. Y. Eom, H. S. Kwon, J. Liu and O. Zhou, *Carbon*, 2004, **42**, 2589.
51 X. X. Wang, J. N. Wang, H. Chang and Y. F. Zhang, *Adv. Funct. Mater.*, 2007, **17**, 3613.
52 C. H. Mi, G. S. Cao and X. B. Zhao, *J. Electroanal. Chem.*, 2004, **562**, 217.
53 J. Eom, D. Kim and H. S. Kwon, *J. Power Sources*, 2006, **157**, 507.
54 R. Lv, L. Zou, X. Gui, F. Kang, Y. Zhu, H. Zhu, J. Wei, J. Gu, K. Wang and D. Wu, *Chem. Commun.*, 2008, 2046.
55 J. S. Zhou, H. H. Song, B. C. Fu, B. Wu and X. H. Chen, *J. Mater. Chem.*, 2010, **20**, 2794.
56 B. J. Lee, J. J. Kim, K. H. Choi, E. C. Shin, W. J. Kim, S. M. Lee and G. H. Jeong, *Surf. Rev. Lett.*, 2010, **17**, 87.
57 S. B. Yang, J. P. Huo, H. H. Song and X. H. Chen, *Electrochim. Acta*, 2008, **53**, 2238.
58 S. H. Ng, J. Wang, Z. P. Guo, G. X. Wang and H. K. Liu, *Electrochim. Acta*, 2005, **51**, 23.
59 J. X. Li, Y. Zhao and L. H. Guan, *Electrochem. Commun.*, 2010, **12**, 592.
60 C. C. Li, X. M. Yin, L. B. Chen, Q. H. Li and T. H. Wang, *J. Phys. Chem. C*, 2009, **113**, 13438.
61 V. Subramanian, H. W. Zhu and B. Q. Wei, *J. Phys. Chem. B*, 2006, **110**, 7178.
62 L. Ji, Z. Lin, A. J. Medford and X. Zhang, *Chem.–Eur. J.*, 2009, **15**, 10718.
63 H. L. Zhang, Y. Zhang, X. G. Zhang, F. Li, C. Liu, J. Tan and H. M. Cheng, *Carbon*, 2006, **44**, 2778.
64 D. Deng and J. Y. Lee, *Chem. Mater.*, 2007, **19**, 4198.
65 L. W. Ji, Z. Lin, R. Zhou, Q. Shi, O. Toprakci, A. J. Medford, C. R. Millns and X. W. Zhang, *Electrochim. Acta*, 2010, **55**, 1605.
66 C. Kim, K. S. Yang, M. Kojima, K. Yoshida, Y. J. Kim, Y. A. Kim and M. Endo, *Adv. Funct. Mater.*, 2006, **16**, 2393.
67 L. Ji, Z. Lin, A. J. Medford and X. Zhang, *Carbon*, 2009, **47**, 3346.
68 L. Ji and X. Zhang, *Nanotechnology*, 2009, **20**, 155705.
69 L. W. Ji, Y. F. Yao, O. Toprakci, Z. Lin, Y. Z. Liang, Q. Shi, A. J. Medford, C. R. Millns and X. W. Zhang, *J. Power Sources*, 2010, **195**, 2050.
70 A. V. Murugan, T. Muraliganth and A. Manthiram, *J. Phys. Chem. C*, 2008, **112**, 14665.
71 E. Yoo, J. Kim, E. Hosono, H. Zhou, T. Kudo and I. Honma, *Nano Lett.*, 2008, **8**, 2277.
72 M. Yoo, C. W. Frank, S. Mori and S. Yamaguchi, *Chem. Mater.*, 2004, **16**, 1945.
73 F. Ji, Y. L. Li, J. M. Feng, D. Su, Y. Y. Wen, Y. Feng and F. Hou, *J. Mater. Chem.*, 2009, **19**, 9063.
74 M. H. Liang and L. J. Zhi, *J. Mater. Chem.*, 2009, **19**, 5871.
75 D. Chen, L. H. Tang and J. H. Li, *Chem. Soc. Rev.*, 2010, **39**, 3157.
76 T. Bhardwaj, A. Antic, B. Pavan, V. Barone and B. D. Fahlman, *J. Am. Chem. Soc.*, 2010, **132**, 12556.
77 D. Y. Pan, S. Wang, B. Zhao, M. H. Wu, H. J. Zhang, Y. Wang and Z. Jiao, *Chem. Mater.*, 2009, **21**, 3136.
78 C. Y. Wang, D. Li, C. O. Too and G. G. Wallace, *Chem. Mater.*, 2009, **21**, 2604.
79 G. X. Wang, X. P. Shen, J. Yao and J. Park, *Carbon*, 2009, **47**, 2049.
80 P. Guo, H. H. Song and X. H. Chen, *Electrochem. Commun.*, 2009, **11**, 1320.
81 P. C. Lian, X. F. Zhu, S. Z. Liang, Z. Li, W. S. Yang and H. H. Wang, *Electrochim. Acta*, 2010, **55**, 3909.
82 G. X. Wang, B. Wang, X. L. Wang, J. Park, S. X. Dou, H. Ahn and K. Kim, *J. Mater. Chem.*, 2009, **19**, 8378.
83 S. Q. Chen, P. Chen, M. H. Wu, D. Y. Pan and Y. Wang, *Electrochem. Commun.*, 2010, **12**, 1302.
84 S. L. Chou, J. Z. Wang, M. Choucair, H. K. Liu, J. A. Stride and S. X. Dou, *Electrochem. Commun.*, 2010, **12**, 303.
85 S. B. Yang, G. L. Cui, S. P. Pang, Q. Cao, U. Kolb, X. L. Feng, J. Maier and K. Mullen, *ChemSusChem*, 2010, **3**, 236.
86 Z. S. Wu, W. C. Ren, L. Wen, L. B. Gao, J. P. Zhao, Z. P. Chen, G. M. Zhou, F. Li and H. M. Cheng, *ACS Nano*, 2010, **4**, 3187.
87 D. H. Wang, D. W. Choi, J. Li, Z. G. Yang, Z. M. Nie, R. Kou, D. H. Hu, C. M. Wang, L. V. Saraf, J. G. Zhang, I. A. Aksay and J. Liu, *ACS Nano*, 2009, **3**, 907.
88 M. Zhang, D. N. Lei, X. M. Yin, L. B. Chen, Q. H. Li, Y. G. Wang and T. H. Wang, *J. Mater. Chem.*, 2010, **20**, 5538.
89 G. M. Zhou, D. W. Wang, F. Li, L. L. Zhang, N. Li, Z. S. Wu, L. Wen, G. Q. Lu and H. M. Cheng, *Chem. Mater.*, 2010, **22**, 5306.
90 H. L. Wang, L. F. Cui, Y. A. Yang, H. S. Casalongue, J. T. Robinson, Y. Y. Liang, Y. Cui and H. J. Dai, *J. Am. Chem. Soc.*, 2010, **132**, 13978.
91 B. Wang, X. L. Wu, C. Y. Shu, Y. G. Guo and C. R. Wang, *J. Mater. Chem.*, 2010, **20**, 10661.
92 J. Yao, X. P. Shen, B. Wang, H. K. Liu and G. X. Wang, *Electrochem. Commun.*, 2009, **11**, 1849.
93 S. M. Paek, E. Yoo and I. Honma, *Nano Lett.*, 2009, **9**, 72.
94 S. W. Woo, K. Dokko, H. Nakano and K. Kanamura, *Electrochemistry*, 2007, **75**, 635.
95 Y. S. Hu, P. Adelhelm, B. M. Smarsly, S. Hore, M. Antonietti and J. Maier, *Adv. Funct. Mater.*, 2007, **17**, 1873.
96 F. Cheng, Z. Tao, J. Liang and J. Chen, *Chem. Mater.*, 2008, **20**, 667.
97 C. J. Meyers, S. D. Shah, S. C. Patel, R. M. Sneeringer, C. A. Bessel, N. R. Dollahon, R. A. Leising and E. S. Takeuchi, *J. Phys. Chem. B*, 2001, **105**, 2143.
98 T. Wang, X. Y. Liu, D. Y. Zhao and Z. Y. Jiang, *Chem. Phys. Lett.*, 2004, **389**, 327.
99 H. S. Zhou, S. M. Zhu, M. Hibino, I. Honma and M. Ichihara, *Adv. Mater.*, 2003, **15**, 2107.
100 F. B. Su, X. S. Zhao, Y. Wang, J. H. Zeng, Z. C. Zhou and J. Y. Lee, *J. Phys. Chem. B*, 2005, **109**, 20200.
101 K. T. Lee, J. C. Lytle, N. S. Ergang, S. M. Oh and A. Stein, *Adv. Funct. Mater.*, 2005, **15**, 547.
102 X. Liu, Y. S. Hu, J. O. Muller, R. Schlogl, J. Maier and D. S. Su, *ChemSusChem*, 2010, **3**, 261.
103 Z. S. Wu, W. C. Ren, L. B. Gao, B. L. Liu, C. B. Jiang and H. M. Cheng, *Carbon*, 2009, **47**, 493.
104 J. Zhang, Y. S. Hu, J. P. Tessonnier, G. Weinberg, J. Maier, R. Schlogl and D. S. Su, *Adv. Mater.*, 2008, **20**, 1450.

105 M. Holzapfel, H. Buqa, W. Scheifele, P. Novak and F. M. Petrat, *Chem. Commun.*, 2005, 1566.
106 C. M. Park, J. H. Kim, H. Kim and H. J. Sohn, *Chem. Soc. Rev.*, 2010, **39**, 3115.
107 W. J. Zhang, *J. Power Sources*, 2011, **196**, 877.
108 T. P. Kumar, R. Ramesh, Y. Y. Lin and G. T. K. Fey, *Electrochem. Commun.*, 2004, **6**, 520.
109 Y. Kwon, H. Kim, S. G. Doo and J. H. Cho, *Chem. Mater.*, 2007, **19**, 982.
110 C. M. Park and H. J. Sohn, *Chem. Mater.*, 2008, **20**, 3169.
111 C. M. Park and H. J. Sohn, *Adv. Mater.*, 2010, **22**, 47.
112 H. C. Shin and M. L. Liu, *Adv. Funct. Mater.*, 2005, **15**, 582.
113 K. K. D. Ehinon, S. Naille, R. Dedryvere, P. E. Lippens, J. C. Jumas and D. Gonbeau, *Chem. Mater.*, 2008, **20**, 5388.
114 J. Hassoun, S. Panero, P. Simon, P. L. Taberna and B. Scrosati, *Adv. Mater.*, 2007, **19**, 1632.
115 J. M. Mosby and A. L. Prieto, *J. Am. Chem. Soc.*, 2008, **130**, 10656.
116 Y. S. Hu, R. Demir-Cakan, M. M. Titirici, J. O. Muller, R. Schlogl, M. Antonietti and J. Maier, *Angew. Chem., Int. Ed.*, 2008, **47**, 1645.
117 R. Teki, M. K. Datta, R. Krishnan, T. C. Parker, T. M. Lu, P. N. Kumta and N. Koratkar, *Small*, 2009, **5**, 2236.
118 X. W. Zhang, P. K. Patil, C. S. Wang, A. J. Appleby, F. E. Little and D. L. Cocke, *J. Power Sources*, 2004, **125**, 206.
119 H. Kim, B. Han, J. Choo and J. Cho, *Angew. Chem., Int. Ed.*, 2008, **47**, 10151.
120 H. Y. Lee and S. M. Lee, *Electrochem. Commun.*, 2004, **6**, 465.
121 G. X. Wang, J. H. Ahn, J. Yao, S. Bewlay and H. K. Liu, *Electrochem. Commun.*, 2004, **6**, 689.
122 W. Wang, M. K. Datta and P. N. Kumta, *J. Mater. Chem.*, 2007, **17**, 3229.
123 T. Zhang, J. Gao, L. J. Fu, L. C. Yang, Y. P. Wu and H. Q. Wu, *J. Mater. Chem.*, 2007, **17**, 1321.
124 H. Kim, M. Seo, M. H. Park and J. Cho, *Angew. Chem., Int. Ed.*, 2010, **49**, 2146.
125 U. Kasavajjula, C. S. Wang and A. J. Appleby, *J. Power Sources*, 2007, **163**, 1003.
126 C. K. Chan, H. L. Peng, G. Liu, K. McIlwrath, X. F. Zhang, R. A. Huggins and Y. Cui, *Nat. Nanotechnol.*, 2008, **3**, 31.
127 H. Ma, F. Y. Cheng, J. Chen, J. Z. Zhao, C. S. Li, Z. L. Tao and J. Liang, *Adv. Mater.*, 2007, **19**, 4067.
128 M. H. Park, M. G. Kim, J. Joo, K. Kim, J. Kim, S. Ahn, Y. Cui and J. Cho, *Nano Lett.*, 2009, **9**, 3844.
129 J. Xiao, W. Xu, D. Y. Wang, D. W. Choi, W. Wang, X. L. Li, G. L. Graff, J. Liu and J. G. Zhang, *J. Electrochem. Soc.*, 2010, **157**, A1047.
130 L. F. Cui, Y. Yang, C. M. Hsu and Y. Cui, *Nano Lett.*, 2009, **9**, 3370.
131 B. Hertzberg, A. Alexeev and G. Yushin, *J. Am. Chem. Soc.*, 2010, **132**, 8548.
132 A. Magasinski, P. Dixon, B. Hertzberg, A. Kvit, J. Ayala and G. Yushin, *Nat. Mater.*, 2010, **9**, 353.
133 N. Dimov, S. Kugino and M. Yoshio, *Electrochim. Acta*, 2003, **48**, 1579.
134 Y. Liu, T. Matsumura, N. Imanishi, A. Hirano, T. Ichikawa and Y. Takeda, *Electrochem. Solid-State Lett.*, 2005, **8**, A599.
135 S. H. Ng, J. Z. Wang, D. Wexler, K. Konstantinov, Z. P. Guo and H. K. Liu, *Angew. Chem., Int. Ed.*, 2006, **45**, 6896.
136 X. L. Yang, Z. Y. Wen, X. J. Zhu and S. H. Huang, *Electrochem. Solid-State Lett.*, 2005, **8**, A481.
137 Y. Zhang, X. G. Zhang, H. L. Zhang, Z. G. Zhao, F. Li, C. Liu and H. M. Cheng, *Electrochim. Acta*, 2006, **51**, 4994.
138 Y. Kwon and J. Cho, *Chem. Commun.*, 2008, 1109.
139 W. J. Lee, M. H. Park, Y. Wang, J. Y. Lee and J. Cho, *Chem. Commun.*, 2010, **46**, 622.
140 M. S. Park, Y. J. Lee, S. Rajendran, M. S. Song, H. S. Kim and J. Y. Lee, *Electrochim. Acta*, 2005, **50**, 5561.
141 M. S. Park, S. Rajendran, Y. M. Kang, K. S. Han, Y. S. Han and J. Y. Lee, *J. Power Sources*, 2006, **158**, 650.
142 H. Kim and J. Cho, *Nano Lett.*, 2008, **8**, 3688.
143 L. W. Ji, K. H. Jung, A. J. Medford and X. W. Zhang, *J. Mater. Chem.*, 2009, **19**, 4992.
144 L. Ji and X. Zhang, *Electrochem. Commun.*, 2009, **11**, 1146.
145 L. Ji and X. Zhang, *Energy Environ. Sci.*, 2010, **3**, 124.
146 G. Armstrong, A. R. Armstrong, P. G. Bruce, P. Reale and B. Scrosati, *Adv. Mater.*, 2006, **18**, 2597.
147 C. S. Fuller and J. C. Severiens, *Phys. Rev.*, 1954, **96**, 21.
148 J. Graetz, C. C. Ahn, R. Yazami and B. Fultz, *J. Electrochem. Soc.*, 2004, **151**, A698.
149 M. Winter and J. O. Besenhard, *Electrochim. Acta*, 1999, **45**, 31.
150 L. C. Yang, Q. S. Gao, L. Li, Y. Tang and Y. P. Wu, *Electrochem. Commun.*, 2010, **12**, 418.
151 C. K. Chan, X. F. Zhang and Y. Cui, *Nano Lett.*, 2008, **8**, 307.
152 H. Lee, M. G. Kim, C. H. Choi, Y. K. Sun, C. S. Yoon and J. Cho, *J. Phys. Chem. B*, 2005, **109**, 20719.
153 X. H. Hou, S. J. Hu and L. Shi, *Acta Phys. Sin.*, 2010, **59**, 2109.
154 H. Li, Q. Wang, L. H. Shi, L. Q. Chen and X. J. Huang, *Chem. Mater.*, 2002, **14**, 103.
155 M. Noh, Y. Kwon, H. Lee, J. Cho, Y. Kim and M. G. Kim, *Chem. Mater.*, 2005, **17**, 1926.
156 M. S. Park, S. A. Needham, G. X. Wang, Y. M. Kang, J. S. Park, S. X. Dou and H. K. Liu, *Chem. Mater.*, 2007, **19**, 2406.
157 Y. Yu, C. H. Chen and Y. Shi, *Adv. Mater.*, 2009, **21**, 3541.
158 H. Lee and J. Cho, *Nano Lett.*, 2007, **7**, 2638.
159 M. G. Kim and J. Cho, *J. Electrochem. Soc.*, 2009, **156**, A277.
160 G. Cui, L. Gu, L. Zhi, N. Kaskhedikar, P. A. V. Aken, K. Müllen and J. Maier, *Adv. Mater.*, 2008, **20**, 3079.
161 G. L. Cui, L. Gu, N. Kaskhedikar, P. A. van Aken and J. Maier, *Electrochim. Acta*, 2010, **55**, 985.
162 K. T. Lee, Y. S. Jung and S. M. Oh, *J. Am. Chem. Soc.*, 2003, **125**, 5652.
163 D. C. S. Souza, V. Pralong, A. J. Jacobson and L. F. Nazar, *Science*, 2002, **296**, 2012.
164 S. Boyanov, M. Womes, L. Monconduit and D. Zitoun, *Chem. Mater.*, 2009, **21**, 3684.
165 F. Gillot, L. Monoconduit, M. Morcrette, M. L. Doublet, L. Dupont and J. M. Tarascon, *Chem. Mater.*, 2005, **17**, 3627.
166 Y. Kim, H. Hwang, C. S. Yoon, M. G. Kim and J. Cho, *Adv. Mater.*, 2007, **19**, 92.
167 H. Hwang, M. G. Kim and J. Cho, *J. Phys. Chem. C*, 2007, **111**, 1186.
168 Y. U. Kim, B. W. Cho and H. J. Sohn, *J. Electrochem. Soc.*, 2005, **152**, A1475.
169 D. C. C. Silva, O. Crosnier, G. Ouvrard, J. Greedan, A. Safa-Sefat and L. F. Nazar, *Electrochem. Solid-State Lett.*, 2003, **6**, A162.
170 H. Hwang, M. G. Kim, Y. Kim, S. W. Martin and J. Cho, *J. Mater. Chem.*, 2007, **17**, 3161.
171 M. P. Bichat, J. L. Pascal, F. Gillot and F. Favier, *Chem. Mater.*, 2005, **17**, 6761.
172 M. V. V. M. S. Kishore and U. V. Varadaraju, *J. Power Sources*, 2006, **156**, 594.
173 S. Boyanov, J. Bernardi, E. Bekaert, M. Menetrier, M. L. Doublet and L. Monconduit, *Chem. Mater.*, 2009, **21**, 298.
174 F. Gillot, S. Boyanov, L. Dupont, M. L. Doublet, A. Morcrette, L. Monconduit and J. M. Tarascon, *Chem. Mater.*, 2005, **17**, 6327.
175 M. P. Bichat, T. Politova, J. L. Pascal, F. Favier and L. Monconduit, *J. Electrochem. Soc.*, 2004, **151**, A2074.
176 O. Crosnier and L. F. Nazar, *Electrochem. Solid-State Lett.*, 2004, **7**, A187.
177 R. Alcantara, J. L. Tirado, J. C. Jumas, L. Monconduit and J. Olivier-Fourcade, *J. Power Sources*, 2002, **109**, 308.
178 V. Pralong, D. C. S. Souza, K. T. Leung and L. F. Nazar, *Electrochem. Commun.*, 2002, **4**, 516.
179 J. T. Vaughey, K. D. Kepler, R. Benedek and M. M. Thackeray, *Electrochem. Commun.*, 1999, **1**, 517.
180 Y. U. Kim, C. K. Lee, H. J. Sohn and T. Kang, *J. Electrochem. Soc.*, 2004, **151**, A933.
181 J. Cabana, L. Monconduit, D. Larcher and M. R. Palacin, *Adv. Mater.*, 2010, **22**, E170.
182 W. X. Chen, J. Y. Lee and Z. L. Liu, *Carbon*, 2003, **41**, 959.
183 S. M. Yoon, K. J. Choi, N. Y. Lee, S. Y. Lee, Y. S. Park and B. G. Yu, *Jpn. J. Appl. Phys.*, 2007, **46**, 7225.
184 X. M. He, W. H. Pu, L. Wang, J. G. Ren, C. Y. Jiang and C. R. Wan, *Electrochim. Acta*, 2007, **52**, 3651.
185 J. Hassoun, G. Derrien, S. Panero and B. Scrosati, *J. Power Sources*, 2008, **183**, 339.
186 C. M. Ionica, P. E. Lippens, J. O. Fourcade and J. C. Jumas, *J. Power Sources*, 2005, **146**, 478.
187 C. Villevieille, B. Fraisse, M. Womes, J. C. Jumas and L. Monconduit, *J. Power Sources*, 2009, **189**, 324.
188 H. Honda, H. Sakaguchi, Y. Fukuda and T. Esaka, *Mater. Res. Bull.*, 2003, **38**, 647.

189 K. C. Hewitt, L. Y. Beaulieu and J. R. Dahn, *J. Electrochem. Soc.*, 2001, **148**, A402.
190 J. T. Vaughey, L. Fransson, H. A. Swinger, K. Edstrom and M. M. Thackeray, *J. Power Sources*, 2003, **119**, 64.
191 S. Grugeon, S. Laruelle, L. Dupont and J. M. Tarascon, *Solid State Sci.*, 2003, **5**, 895.
192 F. J. Fernandez-Madrigal, P. Lavela, C. Perez-Vicente and J. L. Tirado, *J. Electroanal. Chem.*, 2001, **501**, 205.
193 D. Larcher, L. Y. Beaulieu, O. Mao, A. E. George and J. R. Dahn, *J. Electrochem. Soc.*, 2000, **147**, 1703.
194 C. Villevieille, C. M. Ionica-Bousquet, B. Ducourant, J. C. Jumas and L. Monconduit, *J. Power Sources*, 2007, **172**, 388.
195 H. Li, X. J. Huang and L. Q. Chen, *Solid State Ionics*, 1999, **123**, 189.
196 L. F. Nazar, G. Goward, F. Leroux, M. Duncan, H. Huang, T. Kerr and J. Gaubicher, *Int. J. Inorg. Mater.*, 2001, **3**, 191.
197 M. N. Obrovac, R. A. Dunlap, R. J. Sanderson and J. R. Dahn, *J. Electrochem. Soc.*, 2001, **148**, A576.
198 A. Rumplecker, F. Kleitz, E. L. Salabas and F. Schuth, *Chem. Mater.*, 2007, **19**, 485.
199 M. S. Wu and P. C. J. Chiang, *Electrochem. Commun.*, 2006, **8**, 383.
200 W. Yue and W. Z. Zhou, *Chem. Mater.*, 2007, **19**, 2359.
201 L. J. Zhi, Y. S. Hu, B. El Hamaoui, X. Wang, I. Lieberwirth, U. Kolb, J. Maier and K. Mullen, *Adv. Mater.*, 2008, **20**, 1727.
202 Y. Idota, T. Kubota, A. Matsufuji, Y. Maekawa and T. Miyasaka, *Science*, 1997, **276**, 1395.
203 P. Poizot, S. Laruelle, S. Grugeon, L. Dupont and J. Tarascon, *Nature*, 2000, **407**, 496.
204 J. Fan, T. Wang, C. Z. Yu, B. Tu, Z. Y. Jiang and D. Y. Zhao, *Adv. Mater.*, 2004, **16**, 1432.
205 W. Xu, N. L. Canfield, D. Y. Wang, J. Xiao, Z. M. Nie and J. G. Zhang, *J. Power Sources*, 2010, **195**, 7403.
206 I. A. Courtney and J. R. Dahn, *J. Electrochem. Soc.*, 1997, **144**, 2045.
207 W. J. Zhang, *J. Power Sources*, 2011, **196**, 13.
208 M. S. Park, Y. M. Kang, G. X. Wang, S. X. Dou and H. K. Liu, *Adv. Funct. Mater.*, 2008, **18**, 455.
209 J. P. Liu, Y. Y. Li, X. T. Huang, R. M. Ding, Y. Y. Hu, J. Jiang and L. Liao, *J. Mater. Chem.*, 2009, **19**, 1859.
210 Z. Ying, Q. Wan, H. Cao, Z. T. Song and S. L. Feng, *Appl. Phys. Lett.*, 2005, **87**, 113108.
211 Y. L. Zhang, Y. Liu and M. L. Liu, *Chem. Mater.*, 2006, **18**, 4643.
212 D. Deng and J. Y. Lee, *Chem. Mater.*, 2008, **20**, 1841.
213 Z. P. Guo, G. D. Du, Y. Nuli, M. F. Hassan and H. K. Liu, *J. Mater. Chem.*, 2009, **19**, 3253.
214 H. Kim and J. Cho, *J. Mater. Chem.*, 2008, **18**, 771.
215 S. J. Han, B. C. Jang, T. Kim, S. M. Oh and T. Hyeon, *Adv. Funct. Mater.*, 2005, **15**, 1845.
216 X. W. Lou, J. S. Chen, P. Chen and L. A. Archer, *Chem. Mater.*, 2009, **21**, 2868.
217 X. M. Sun, J. F. Liu and Y. D. Li, *Chem. Mater.*, 2006, **18**, 3486.
218 H. X. Zhang, C. Feng, Y. C. Zhai, K. L. Jiang, Q. Q. Li and S. S. Fan, *Adv. Mater.*, 2009, **21**, 2299.
219 X. W. Lou, C. M. Li and L. A. Archer, *Adv. Mater.*, 2009, **21**, 2536.
220 Y. Wang, H. C. Zeng and J. Y. Lee, *Adv. Mater.*, 2006, **18**, 645.
221 L. Ji, Z. Lin, B. Guo, A. J. Medford and X. Zhang, *Chem.–Eur. J.*, 2010, **16**, 11543.
222 Y. G. Guo, Y. S. Hu and J. Maier, *Chem. Commun.*, 2006, 2783.
223 Y. G. Guo, Y. S. Hu, W. Sigle and J. Maier, *Adv. Mater.*, 2007, **19**, 2087.
224 K. Saravanan, K. Ananthanarayanan and P. Balaya, *Energy Environ. Sci.*, 2010, **3**, 939.
225 K. X. Wang, M. D. Wei, M. A. Morris, H. S. Zhou and J. D. Holmes, *Adv. Mater.*, 2007, **19**, 3016.
226 J. J. Auborn and Y. L. Barberio, *J. Electrochem. Soc.*, 1987, **134**, 638.
227 A. K. Sleigh and W. R. Mckinnon, *Solid State Ionics*, 1991, **45**, 67.
228 P. Adelhelm, Y. S. Hu, M. Antonietti, J. Maier and B. M. Smarsly, *J. Mater. Chem.*, 2009, **19**, 1616.
229 D. Larcher, C. Masquelier, D. Bonnin, Y. Chabre, V. Masson, J. B. Leriche and J. M. Tarascon, *J. Electrochem. Soc.*, 2003, **150**, A133.
230 M. V. Reddy, T. Yu, C. H. Sow, Z. X. Shen, C. T. Lim, G. V. S. Rao and B. V. R. Chowdari, *Adv. Funct. Mater.*, 2007, **17**, 2792.
231 J. Morales, L. Sanchez, F. Martin, F. Berry and X. L. Ren, *J. Electrochem. Soc.*, 2005, **152**, A1748.
232 J. Chen, L. N. Xu, W. Y. Li and X. L. Gou, *Adv. Mater.*, 2005, **17**, 582.
233 S. L. Liu, L. N. Zhang, J. P. Zhou, J. F. Xiang, J. T. Sun and J. G. Guan, *Chem. Mater.*, 2008, **20**, 3623.
234 J. Hu, H. Li, X. J. Huang and L. Q. Chen, *Solid State Ionics*, 2006, **177**, 2791.
235 J. Jamnik and J. Maier, *Phys. Chem. Chem. Phys.*, 2003, **5**, 5215.
236 J. S. Zhou, H. H. Song, X. H. Chen, L. J. Zhi, S. Y. Yang, J. P. Huo and W. T. Yang, *Chem. Mater.*, 2009, **21**, 2935.
237 W. M. Zhang, X. L. Wu, J. S. Hu, Y. G. Guo and L. J. Wan, *Adv. Funct. Mater.*, 2008, **18**, 3941.
238 Z. M. Cui, L. Y. Hang, W. G. Song and Y. G. Guo, *Chem. Mater.*, 2009, **21**, 1162.
239 C. H. Chen, B. J. Hwang, J. S. Do, J. H. Weng, M. Venkateswarlu, M. Y. Cheng, R. Santhanam, K. Ragavendran, J. F. Lee, J. M. Chen and D. G. Liu, *Electrochem. Commun.*, 2010, **12**, 496.
240 K. M. Shaju, F. Jiao, A. Debart and P. G. Bruce, *Phys. Chem. Chem. Phys.*, 2007, **9**, 1837.
241 F. M. Zhan, B. Y. Geng and Y. J. Guo, *Chem.–Eur. J.*, 2009, **15**, 6169.
242 Y. G. Li, B. Tan and Y. Y. Wu, *Nano Lett.*, 2008, **8**, 265.
243 X. W. Lou, D. Deng, J. Y. Lee, J. Feng and L. A. Archer, *Adv. Mater.*, 2008, **20**, 258.
244 Y. Shan and L. Gao, *Chem. Lett.*, 2004, **33**, 1560.
245 N. Du, H. Zhang, B. Chen, J. B. Wu, X. Y. Ma, Z. H. Liu, Y. Q. Zhang, D. Yang, X. H. Huang and J. P. Tu, *Adv. Mater.*, 2007, **19**, 4505.
246 W. Y. Li, L. N. Xu and J. Chen, *Adv. Funct. Mater.*, 2005, **15**, 851.
247 P. Zhang, Z. P. Guo, S. G. Kang, Y. J. Choi, C. J. Kim, K. W. Kim and H. K. Liu, *J. Power Sources*, 2009, **189**, 566.
248 Y. Yu, C. H. Chen, J. L. Shui and S. Xie, *Angew. Chem., Int. Ed.*, 2005, **44**, 7085.
249 F. Li, Q. Q. Zou and Y. Y. Xia, *J. Power Sources*, 2008, **177**, 546.
250 H. Qiao, L. F. Xiao, Z. Zheng, H. W. Liu, F. L. Jia and L. Z. Zhang, *J. Power Sources*, 2008, **185**, 486.
251 P. Lavela, J. L. Tirado and C. Vidal-Abarca, *Electrochim. Acta*, 2007, **52**, 7986.
252 X. J. Liu, H. Yasuda and M. Yamachi, *J. Power Sources*, 2005, **146**, 510.
253 Q. Fan and M. S. Whittingham, *Electrochem. Solid-State Lett.*, 2007, **10**, A48.
254 D. Pasero, N. Reeves and A. R. West, *J. Power Sources*, 2005, **141**, 156.
255 M. J. Aragon, C. Perez-Vicente and J. L. Tirado, *Electrochem. Commun.*, 2007, **9**, 1744.
256 P. Poizot, S. Laruelle, S. Grugeon and J. M. Tarascon, *J. Electrochem. Soc.*, 2002, **149**, A1212.
257 K. F. Zhong, X. Xia, B. Zhang, H. Li, Z. X. Wang and L. Q. Chen, *J. Power Sources*, 2010, **195**, 3300.
258 M. M. Thackeray, C. S. Johnson, J. T. Vaughey, N. Li and S. A. Hackney, *J. Mater. Chem.*, 2005, **15**, 2257.
259 Y. Yang, D. Shu, H. Yu, X. Xia and Z. G. Lin, *J. Power Sources*, 1997, **65**, 227.
260 K. Zhong, X. Xia, B. Zhang, H. Li, Z. Wang and L. Chen, *J. Power Sources*, 2009, **195**, 3300.
261 M. M. Thackeray, *Prog. Solid State Chem.*, 1997, **25**, 1.
262 X. Q. Yu, Y. He, J. P. Sun, K. Tang, H. Li, L. Q. Chen and X. J. Huang, *Electrochem. Commun.*, 2009, **11**, 791.
263 Q. Fan, P. J. Chupas and M. S. Whittingham, *Electrochem. Solid-State Lett.*, 2007, **10**, A274.
264 M. S. Wu, P. C. J. Chiang, J. T. Lee and J. C. Lin, *J. Phys. Chem. B*, 2005, **109**, 23279.
265 Y. Y. Yang, Y. Q. Zhao, L. F. Xiao and L. Z. Zhang, *Electrochem. Commun.*, 2008, **10**, 1117.
266 L. Ji and X. Zhang, *Electrochem. Commun.*, 2009, **11**, 795.
267 L. Ji, A. J. Medford and X. Zhang, *J. Mater. Chem.*, 2009, **19**, 5593.
268 Z. Lin, L. W. Ji, M. D. Woodroof and X. W. Zhang, *J. Power Sources*, 2010, **195**, 5025.
269 X. L. Ji, S. Herle, Y. H. Rho and L. F. Nazar, *Chem. Mater.*, 2007, **19**, 374.
270 H. Li, P. Balaya and J. Maier, *J. Electrochem. Soc.*, 2004, **151**, A1878.
271 F. Leroux, G. R. Goward, W. P. Power and L. F. Nazar, *Electrochem. Solid-State Lett.*, 1998, **1**, 255.
272 F. Leroux and L. F. Nazar, *Solid State Ionics*, 2000, **133**, 37.

273 S. H. Lee, Y. H. Kim, R. Deshpande, P. A. Parilla, E. Whitney, D. T. Gillaspie, K. M. Jones, A. H. Mahan, S. B. Zhang and A. C. Dillon, *Adv. Mater.*, 2008, **20**, 3627.
274 S. H. Lee, R. Deshpande, D. Benhammou, P. A. Parilla, A. H. Mahan and A. C. Dillon, *Thin Solid Films*, 2009, **517**, 3591.
275 M. F. Hassan, Z. P. Guo, Z. Chen and H. K. Liu, *J. Power Sources*, 2010, **195**, 2372.
276 Y. F. Shi, B. K. Guo, S. A. Corr, Q. H. Shi, Y. S. Hu, K. R. Heier, L. Q. Chen, R. Seshadri and G. D. Stucky, *Nano Lett.*, 2009, **9**, 4215.
277 P. Balaya, H. Li, L. Kienle and J. Maier, *Adv. Funct. Mater.*, 2003, **13**, 621.
278 H. B. Wang, Q. M. Pan, H. W. Zhao, G. P. Yin and P. J. Zuo, *J. Power Sources*, 2007, **167**, 206.
279 J. C. Park, J. Kim, H. Kwon and H. Song, *Adv. Mater.*, 2009, **21**, 803.
280 L. Fu, J. Gao, T. Zhang, Q. Cao, L. C. Yang, Y. P. Wu and R. Holze, *J. Power Sources*, 2007, **171**, 904.
281 S. F. Zheng, J. S. Hu, L. S. Zhong, W. G. Song, L. J. Wan and Y. G. Guo, *Chem. Mater.*, 2008, **20**, 3617.
282 A. Debart, L. Dupont, P. Poizot, J. B. Leriche and J. M. Tarascon, *J. Electrochem. Soc.*, 2001, **148**, A1266.
283 S. Grugeon, S. Laruelle, R. Herrera-Urbina, L. Dupont, P. Poizot and J. M. Tarascon, *J. Electrochem. Soc.*, 2001, **148**, A285.
284 J. Morales, L. Sanchez, F. Martin, J. R. Ramos-Barrado and M. Sanchez, *Electrochim. Acta*, 2004, **49**, 4589.
285 Y. G. Li, B. Tan and Y. Y. Wu, *Chem. Mater.*, 2008, **20**, 2602.
286 F. S. Ke, L. Huang, G. Z. Wei, L. J. Xue, J. T. Li, B. Zhang, S. R. Chen, X. Y. Fan and S. G. Sun, *Electrochim. Acta*, 2009, **54**, 5825.
287 L. B. Chen, N. Lu, C. M. Xu, H. C. Yu and T. H. Wang, *Electrochim. Acta*, 2009, **54**, 4198.
288 X. P. Gao, J. L. Bao, G. L. Pan, H. Y. Zhu, P. X. Huang, F. Wu and D. Y. Song, *J. Phys. Chem. B*, 2004, **108**, 5547.
289 J. Y. Xiang, J. P. Tu, Y. F. Yuan, X. L. Wang, X. H. Huang and Z. Y. Zeng, *Electrochim. Acta*, 2009, **54**, 1160.
290 H. Huang, E. M. Kelder and J. Schoonman, *J. Power Sources*, 2001, **97–98**, 114.
291 G. T. Wu, C. S. Wang, X. B. Zhang, H. S. Yang, Z. F. Qi and W. Z. Li, *J. Power Sources*, 1998, **75**, 175.
292 J. Y. Xiang, J. P. Tu, Y. F. Yuan, X. H. Huang, Y. Zhou and L. Zhang, *Electrochem. Commun.*, 2009, **11**, 262.
293 Y. H. Lee, I. C. Leu, S. T. Chang, C. L. Liao and K. Z. Fung, *Electrochim. Acta*, 2004, **50**, 553.
294 Y. H. Lee, I. C. Leu, C. L. Liao, S. T. Chang, M. T. Wu, J. H. Yen and K. Z. Fung, *Electrochem. Solid-State Lett.*, 2006, **9**, A207.
295 L. Fu, J. Gao, T. Zhang, Q. Cao, L. C. Yang, Y. P. Wu, R. Holze and H. Q. Wu, *J. Power Sources*, 2007, **174**, 1197.
296 J. Y. Xiang, X. L. Wang, X. H. Xia, L. Zhang, Y. Zhou, S. J. Shi and J. P. Tu, *Electrochim. Acta*, 2010, **55**, 4921.
297 Y. Yu, Y. Shi and C. H. Chen, *Nanotechnology*, 2007, **18**, 055706.
298 Q. M. Pan, M. Wang and Z. J. Wang, *Electrochem. Solid-State Lett.*, 2009, **12**, A50.
299 J. Hu, H. Li and X. J. Huang, *Electrochem. Solid-State Lett.*, 2005, **8**, A66.
300 I. Ayub, F. J. Berry, C. Johnson, D. A. Johnson, E. A. Moore, X. L. Ren and H. M. Widatallah, *Solid State Commun.*, 2002, **123**, 141.
301 A. Holt and P. Kofstad, *Solid State Ionics*, 1997, **100**, 201.
302 A. Holt and P. Kofstad, *Solid State Ionics*, 1999, **117**, 21.
303 X. H. Huang, J. P. Tu, C. Q. Zhang and J. Y. Xiang, *Electrochem. Commun.*, 2007, **9**, 1180.
304 Y. F. Yuan, X. H. Xia, J. B. Wu, J. L. Yang, Y. B. Chen and S. Y. Guo, *Electrochem. Commun.*, 2010, **12**, 890.
305 O. Delmer, P. Balaya, L. Kienle and J. Maier, *Adv. Mater.*, 2008, **20**, 501.
306 S. H. Choi, J. S. Kim and Y. S. Yoon, *Electrochim. Acta*, 2004, **50**, 547.
307 Y. A. Jeon, K. S. No, S. H. Choi, J. P. Ahn and Y. S. Yoon, *Electrochim. Acta*, 2004, **50**, 907.
308 A. Debart, L. Dupont, R. Patrice and J. M. Tarascon, *Solid State Sci.*, 2006, **8**, 640.
309 T. Takeuchi, H. Sakaebe, H. Kageyama, T. Sakai and K. Tatsumi, *J. Electrochem. Soc.*, 2008, **155**, A679.
310 J. M. Yan, H. Z. Huang, J. Zhang, Z. J. Liu and Y. Yang, *J. Power Sources*, 2005, **146**, 264.
311 C. Q. Feng, L. F. Huang, Z. P. Guo and H. K. Liu, *Electrochem. Commun.*, 2007, **9**, 119.
312 J. Xiao, D. W. Choi, L. Cosimbescu, P. Koech, J. Liu and J. P. Lemmon, *Chem. Mater.*, 2010, **22**, 4522.
313 G. X. Wang, S. Bewlay, J. Yao, H. K. Liu and S. X. Dou, *Electrochem. Solid-State Lett.*, 2004, **7**, A321.
314 R. D. Apostolova, E. M. Shembel, I. Talyosef, J. Grinblat, B. Markovsky and D. Aurbach, *Russ. J. Electrochem.*, 2009, **45**, 311.
315 J. Z. Wang, G. X. Wang, L. Yang, S. H. Ng and H. K. Liu, *J. Solid State Electrochem.*, 2006, **10**, 250.
316 B. T. Hang, T. Ohnishi, M. Osada, X. X. Xu, K. Takada and T. Sasaki, *J. Power Sources*, 2010, **195**, 3323.
317 H. Senoh, T. Takeuchi, H. Kageyama, H. Sakaebe, M. Yao, K. Nakanishi, T. Ohta, T. Sakai and K. Yasuda, *J. Power Sources*, 2010, **195**, 8327.
318 J. L. C. Rowsell, V. Pralong and L. F. Nazar, *J. Am. Chem. Soc.*, 2001, **123**, 8598.
319 S. H. Elder, L. H. Doerrer, F. J. Disalvo, J. B. Parise, D. Guyomard and J. M. Tarascon, *Chem. Mater.*, 1992, **4**, 928.
320 J. Cabana, N. Dupre, C. P. Grey, G. Subias, M. T. Caldes, A. M. Marie and M. R. Palacin, *J. Electrochem. Soc.*, 2005, **152**, A2246.
321 M. Nishijima, N. Tadokoro, Y. Takeda, N. Imanishi and O. Yamamoto, *J. Electrochem. Soc.*, 1994, **141**, 2966.
322 T. Shodai, S. Okada, S. Tobishima and J. Yamaki, *Solid State Ionics*, 1996, **86–88**, 785.
323 Q. Sun, W. J. Li and Z. W. Fu, *Solid State Sci.*, 2010, **12**, 397.
324 N. Pereira, L. C. Klein and G. G. Amatucci, *J. Electrochem. Soc.*, 2002, **149**, A262.
325 N. Pereira, M. Balasubramanian, L. Dupont, J. McBreen, L. C. Klein and G. G. Amatucci, *J. Electrochem. Soc.*, 2003, **150**, A1118.
326 L. Baggetto, N. A. M. Verhaegh, R. A. H. Niessen, F. Roozeboom, J. C. Jumas and P. H. L. Notten, *J. Electrochem. Soc.*, 2010, **157**, A340.
327 Q. Sun and Z. W. Fu, *Electrochim. Acta*, 2008, **54**, 403.
328 J. M. Tarascon, *Philos. Trans. R. Soc. London, Ser. A*, 2010, **368**, 3227.
329 D. S. Su and R. Schlügl, *ChemSusChem*, 2010, **3**, 136.
330 X. P. Gao and H. X. Yang, *Energy Environ. Sci.*, 2010, **3**, 174.
331 L. Ji, Z. Tan, T. Kuykendall, S. Aloni, S. Xun, E. Lin, V. Battaglia and Y. Zhang, *Phys. Chem. Chem. Phys.*, 2011, **13**, 7170.